Did the weather in the stratosphere influence the weather in the troposphere in Kiruna during the winter 2002/2003?

Alla Belova

IRF Internal Note 038
September 2003

INSTITUTET FÖR RYMDFYSIK Kiruna
Swedish Institute of Space Physics Sweden

Did the weather in the stratosphere influence the weather in the troposphere in Kiruna during the winter 2002/2003?

Alla Belova
Swedish Institute of Space Physics
24 September 2003

IRF Internal Note 038

Printed in Sweden
Swedish Institute of Space Physics
2003-09-24

Introduction

In the winter period of December 2002 - February 2003 unusually warm days with thaw were observed at locations around Kiruna, 200 km north of the Polar Circle. The task of this work is to try to find out the cause of this unusual weather. In similar works **[1, 2, 3]** it was earlier shown that the North Atlantic (NAO) and the Arctic Oscillation (AO) in the winter period, when the tropospheric and stratospheric circulation are coupled, influences the weather in the extra-tropical Northern Hemisphere. In this work we check the possible interconnection between warm weather in the Kiruna region and the above mentioned effect in the troposphere-stratosphere coupling.

The NAO may be regarded as the manifestation of the AO in the Atlantic sector, and maps of the AO and the NAO over the Atlantic half of the Northern Hemisphere are nearly the same **[1].** In this work the AO only is examined because it has a broader center of action over the polar cap than the NAO and it shows a nearly identical pattern to the NAO in middle to high latitudes from North America to Europe **[1].**

The AO was first defined by *Thomson and Wallace* [1998] as the leading mode of variability of the northern winter sea-level pressure (SLP). They used an empirical orthogonal function (EOF) analysis of wintertime monthly-mean 1000 hPa geopotential anomalies to obtain this leading mode. They called the leading EOF of SLP the Arctic Oscillation. Other words, the leading principal component of the time series is the AO index. The AO is the dominant pattern of non-seasonal sea-level pressure variations north of 20ºN, and it is characterized by SLP anomalies of one sign in the Arctic and anomalies of opposite sign centred about 37º- 45ºN latitude.

Since the 1960s the AO has experienced a “trend” toward a positive index, possibly related to climate change. The changes in the AO at the Earth’s surface have been paralleled by a tendency for the high-latitude stratospheric polar vortex to be stronger and colder. The AO in the troposphere is strongly coupled to the strength of the stratospheric polar vortex, and stratospheric circulation anomalies are seen to propagate downward to the Earth’s surface, where they are seen as changes in the magnitude and sign of the AO **[1].** Since the AO modulates the circulation of the northern troposphere, and even influences low latitudes, intra-seasonal changes in the stratospheric circulation are observed to precede both high and low latitude Atlantic climate anomalies and significant weather events **[3].**

PART 1
Available Data Set and Techniques of Analysis

We use UKMO meteorological data (United Kingdom Met Office, http://www.meto.govt.uk) of temperature and geopotential height at 8 levels (1000 mb, 460 mb, 320 mb, 100 mb, 46 mb, 32 mb, 10 mb, 3.2 mb). These levels were taken in order to study the stratosphere-troposphere coupling. The UKMO-data are daily 12 UT values on a 2.5°x3.75° grid in latitude (73 points) and in longitude (96 points). We use data for the North Hemisphere for the winter period December 2002 - February 2003 (90 days). Temperature and pressure data from Abisko Scientific Research Station (www.ans.kiruna.se) (68ºN21´, 18ºE49´) were taken for this analysis as well. The Abisko station is located at 385 m above the sea-level and we consider this level as1000 mb pressure level.

Because there are no data at Abisko at higher altitudes than the 1000 mb level we have selected data from the UKMO data base at the nearest point to Abisko on the geographical grid at the levels of 460 mb, 320 mb, 100 mb, 46 mb, 32 mb, 10 mb, 3.2 mb.
The maximum of the correlation function for the geopotential at 1000 mb between Abisko (68ºN21´, 18ºE49´) and the nearest UKMO-point 67ºN30´, 18ºE45´ is very high, R=0.98 (the 95% confidence interval is 0.97<**0.98**≤0.99).
The correlation coefficient for temperature data between Abisko and the nearest UKMO-point is equal to 0.84 (0.78<**0.84**<0.89) **(Fig.1).** In addition upper air temperature data from Esrange (67ºN53´, 21ºE06´) were available for the period 15-30 January 2003 when radiosonde and sounding-rocket experiments were conducted.

Fig.1 illustrates the comparison of temperature measurements at 1000 mb, 460 mb, 320 mb and 100 mb. At all altitudes the blue line is the temperature at the UKMO point; the red line is the temperature from radiosondes/sounding rocket at Esrange. The green line is the temperature at Abisko-station at 1000 mb pressure level. **Fig.2** demonstrates the temperature measurements at 46 mb, 32 mb, 10 mb and 3.2 mb. The colours are the same as in **Fig.1**.
These pictures show that at all levels the temperature variations by the UKMO and by radiosondes/rocket data have a good coincidence in both temporal changes and in absolute values. At the same time Abisko and UKMO data at 1000 mb are not as well correlated, R=0.84 (0.78<**0.84**<0.89). This probably due to the inability of the UKMO data to resolve the usual wintertime temperature inversions close to the ground.
The temperature variations around Abisko at 1000 mb - 3.2 mb levels for the period of December 2002 – February 2003 are shown in **Fig.3.**

The AO signature definition
Here we follow the AO signature definition given in [**1**]. The AO signature is derived from the empirical orthogonal function (EOF) analysis. The purpose of EOF is to reduce a data set containing a large number of variables to a data set containing fewer new variables, but that nevertheless represents a large fraction of the variability contained in the original data [**4**]. EOFs are based on analysis of the variance-covariance matrix **[S]**. This matrix contains the sample variance of the K elements of the data vector **x** on its diagonal, and the covariances among these variables in the off-diagonal positions. Thus, **[S]** contains a wealth of information about the nature of the multiple variations exhibited by *x*. In our case vector **x** is the geopotential height **h** and the *K* is the number of geographical points (720) at one level.
EOFs are based on a vector of anomalies **h'.** An anomaly h'_k is obtained by subtracting the sample mean of the h_k values. The new variables, u_m, that will account successively for the maximum amount of the joint variability of **h'** (and therefore also of **h**) are found using the eigenvectors of **[S].** In

particular, the *m*th **principal component, $\mathbf{u_m}$**, is obtained as the projection of the data vector **h'** onto the *m*th eigenvector, e_m,

$$u_m = \mathbf{e}^T_{mx}\,\mathbf{h'} = \Sigma_{k=1}\, e_{km}\, h'_k, \qquad m = 1....M.$$

The overwhelming majority of applications of the EOF analysis to atmospheric data have involved analysis of field (i.e. spatial array of variables) such as geopotential heights and temperatures. In this case the full data set consists of multiple observations of field or of set of fields. And the **principal components** will be **$\mathbf{u_m(t)}$** as the following:

$$u_m(t) = \mathbf{e}^T_{mx}\,\mathbf{h'} = \Sigma_{k=1}\, e_{km}\, h'_k(t), \qquad m = 1....M.$$

Here the time index *t* runs from 1 to 90 days. Geometrically, the first eigenvector, **$\mathbf{e_1}$**, points to the direction (in the K-dimensional space of **h'**) in which the data vectors jointly exhibit the most variability. The first principal components (or the leading EOF) **$\mathbf{u_1(t)}$** according to the first eigenvector **$\mathbf{e_1}$** will be AO indexes. In our case there are 90 AO indexes because of we take a 90 day period.

In this work four different techniques were applied to derive a spatial AO signature.

a) (Fig.4.1.a-4.8.a) First EOFs were calculated **separately** for each of the 8 levels using daily values on a 5ºx7.5º grid in latitude (15 points) and in longitude (48 points) around the North Hemisphere from 20ºN to 90ºN for 90 days (December 2002 - February 2003). The total number of geographical points in the grid is 720.
The AO pattern for each geopotential level was identified as the leading EOF of the temporal (90 days) covariance matrix (720x720) for the same level. From this matrix we obtained the first principal components (or AO indexes). These values were normalized by the standard deviation of the AO index and thus the normalized AO indexes were derived (90 AO indexes, one AO index for each of 90 days). Then the procedure of linear regression between the AO normalized indexes and geopotential anomalies at each of the 720 points was applied.
So, there are 8 geopotential levels and 8 different collections of AO indexes. The spatial signature of the Arctic Oscillation are plotted in **Fig.4.1.a-4.8.a** where the contour value are meters, corresponding to a one standard deviation of geopotential anomaly in the AO index.

b) (Fig.4.1.b-4.8.b) As the AO indexes at 1000 mb have been found (in case **a)**) it was possible to apply a regression between these AO indexes at 1000 mb and the geopotential anomaly at each level. The spatial signature of the Arctic Oscillation is shown in **(Fig.4.1.b-4.8.b),** where the contour value are meters, corresponding to one standard deviation of geopotential anomaly in the AO index. We called these AO indexes **"AO_1000".**

c) (Fig.4.1.c-4.8.c) The first EOF was calculated from a **single field** consisting of five geopotential levels (1000 mb, 460 mb, 100 mb, 46 mb, 10 mb). At each altitude the data are daily values on a 5ºx15º grid in latitude (15 points) and in longitude (24 points) around the North Hemisphere from 20ºN to 90ºN for 90 days (December 2002 - February 2003). The number of points at each level is 360 and the total number of points is 360x5 = 1800.
The AO pattern for all 5 geopotential levels was identified as the leading EOF of the temporal (90 days) covariance matrix (1800x1800). The procedure for AO indexes calculation is the same as in the case **a).** We called these AO indexes **"mean AO indexes"** because they were calculated using data of 5 levels simultaneously. Finally the regression analysis between mean AO normalized indexes and geopotential anomaly in each of 720 points was applied (as in cases **a)** and **b)**).

Filtered data technique

d) (Fig.4.1.d-4.8.d) To exclude the influence of physical and statistical noise an 8-day low pass filter was applied to all geopotential data before mean AO indexes in case **c)** were calculated. We have got

approximately the same structures as in case **c).** It is obvious for this sample the resulting pictures of AO signatures are not sensitive to the technique of calculations with filtered data.

So four different techniques were applied to analyze the data sets and we got three different patterns of the AO signature. Each of them shows signs of troposphere-stratosphere coupling to some extent.

If we consider case **c)** first (ie EOF calculated for all levels simultaneously) we see a steady change in the spatial pattern of the AO progressing from one level to the next. At 1000 mb the main features are a "high" in the north Atlantic and "lows" in the area of Alaska and in the sought Atlantic. Progressing upward to 460 mb and 320 mb, the high over the north Atlantic moves westward over north America while the two lows over Alaska moves north and west towards Siberia and low over the south Atlantic moves north and east towards Europe. Progressing further up in the height, the two lows merge together stretching from Europe over the north pole to Siberia while the high remains rather stable over northernmost America. This same pattern can be seen in the case a) (ie EOF calculated for each level separately) with the notable exception of the 320 mb and 460 mb levels, which show completely different patterns.
Case **b)** (regressions at each level with the AO at 1000 mb) shows also a steady progression from two lows with a high between to a single low over the polar area. Altogether, the steady change of pattern between different levels indeed suggests that the variability characterized by the AO is coupled throughout the height interval. It seems likely that the anomalous results for case **a)** at 320 mb and 460 mb are due to some particular weather pattern which occurred just during the period of our analysis, and which masks the true AO signature.
The correlation analysis between AO indexes in cases **a)** (indexes were calculated separately for each level) and **c)** (indexes were calculated for a single field at 1000 mb - 10 mb) demonstrates that the best correlation coefficient is equal to 0.99 ($0.98<\mathbf{0.99}\leq 0.99$) at the 10 mb level. It means that the geopotential anomalies at 10 mb contribute mainly to the calculation of the mean AO indexes. This is due to the largest anomalies taking place at 10 mb that results in high correlation at this level.

The correlation coefficients between cases **a)** and **c)** for each level are listed in the following **Table 1**:

Height, mb	Correlation coefficient with 95% confidence interval
1000	$0.22<\mathbf{0.41}<0.57$
460	$0.05<\mathbf{0.25}<0.43$
320	$-0.03<\mathbf{0.18}<0.37$
100	$0.31<\mathbf{0.49}<0.63$
46	$0.63<\mathbf{0.74}<0.82$
32	$0.77<\mathbf{0.84}<0.89$
10	$0.98<\mathbf{0.99}\leq 0.99$

In **Tables 2-9** we give a comparison between the AO spatial signature in this work (cases **a), b)** and **c)**) calculated only for one winter period (December 2002 – February 2003) using unfiltered data) and the AO pattern from paper **[1]** (that was calculated for the winter time for period 1958-1997, using 90-day low-pass-filtered data and considering all geopotential levels as a single field).

Below the obtained results of AO signatures at 1000 mb are summarized in **Table 2**.
MAX is the maximal value, corresponding to one standard deviation of geopotential anomaly in the AO index .

Table 2. AO signature at 1000 mb level

	AO pattern by paper [1]	**a) and b) [Our AO] (Fig. 4.1.ab)**	**c) [Our mean AO] (Fig. 4.1.c)**
Location of **negative** centres	over the Arctic region displaced towards Greenland	one strong centre is located above the Arctic region near Canada Basin, Alaska, Beaufort Sea and Chukchi Sea. (MAX= -88); two weak negative centers are situated over Azores and Iberian basin (MAX = -40) and Kazahstan (MAX = -30)	one negative centre with a wide belt is seen over north Canada and Canada Basin (MAX= - 64), another one is over the south Atlantic (from the USA to Spain and France) (MAX = - 45).
MAX, m	**- 45**	**-88, -40, -30**	**-64, -45**
Location of **positive** centres	at midlatitudes with prominent features over the Atlantic and Pacific Oceans	one strong positive centre is located over Iceland (MAX = 75) with weak features over Greenland and Baffin island (MAX = 40) ; two weak centres: one is over China along the south-north azimuth and another one is above the north part of the Pacific Ocean (MAX= 15).	three positive centers of action are located over: Iceland, Spitsbergen (MAX = 25) and over the north part of the Pacific Ocean (MAX= 45).
MAX, m	**25**	**75, 40, 15**	**25, 45**

The main difference between the AO structure of paper **[1]** and case **ab) (Fig. 4.1.ab)** is the shift (in case **ab)**) of the strongest negative center from the north cap to 70º-80º north latitudes and to 120º-150º west longitudes. The positive centers have approximately the same position as in paper **[1]**. The positive and negative geopotential deviations in case **ab) (Fig. 4.1.ab)** are stronger compared to those of [**1**]. Case **c)** is similar to case **ab) (Fig. 4.1.ab)** except for one negative centre over Kazahstan which appears in case **ab)**.

The following **Table 3** demonstrates features of the AO signatures at 460 mb.

Table 3. AO signature at 460 mb level

	AO pattern by paper [1] at 500 mb	**a) [Our AO] at 460 mb (Fig. 4.2.a)**	**b) [Our AO_1000 at 460 mb] (Fig. 4.2.b)**	**c) [Our mean AO at 460 mb] (Fig. 4.1.c)**
Location of **negative** centres	Two negative centeres of action are located over the southern Greenland (MAX = - 60) and the polar cap	The negative centre is located over North Canada (MAX = - 65), Arctic Ocean, in midlatitudes over the Atlantic Ocean	The structure is similar to AO structure at 1000 mb of case **ab) (Fig. 4.1.ab)**	The structure is close to one of case **ab)** at 1000 mb **(Fig. 4.1.ab)** and is close to one of case **b)** at 460 mb **(Fig. 4.2.b)**
MAX, m	**- 60**	**-65**	**-112**	**-85**
Location of **positive** centres	The broad positive midlatitude band (MAX = 30) is over the Atlantic and Pacific Oceans	Strong positive centeres are located: over Spitsbergen (MAX = 160), over the north of Scandinavian, Norwegian, Barents and Greenland Seas. There is weak broad midlatitude positive band (MAX = 40) over the Pacific Ocean, Michigan area in the USA and over Morocco.	The structure is similar to AO structure at 1000 mb of case **ab) (Fig. 4.1.ab)**	The structure is close to one of case **ab)** at 1000 mb **(Fig. 4.1.ab)** and is close to one of case **b)** at 460 mb **(Fig. 4.2.b)**
MAX, m	**30**	**160**	**100**	**85**

The main difference between the AO structure of paper **[1]** and case **a)** is that there is the shift (in case **a)**) of the strongest positive center from midlatitudes to the north pole and its geopotential deviation is stronger. The negative centers have approximately the same locations and the same deviations.

The following **Table 4** illustrates characteristics of the AO signatures at 300 mb.

Table 4. AO signature at 300 mb level

	AO pattern by paper [1] at 300 mb	**a) [Our AO] at 320 mb (Fig. 4.3.a)**	**b) [Our AO_1000 at 320 mb] (Fig. 4.3.b)**	**c) [Our mean AO at 320 mb] (Fig. 4.3.c)**
Location of **negative** and **positive** centres	The structure is similar to AO structure at 500 mb of [**1**]	The same structure as in case **a)** at 460 mb **(Fig. 4.2.a)**	The structure is similar to one of case **b)** at 460 mb **(Fig. 4.2.6)** and at 1000 mb **(Fig. 4.1.ab)**	The structure is close to one of case **c)** at 460 mb **(Fig. 4.2.c)**
MAX, m	**-90**	**-64**	**-128**	**-103**
MAX, m	**45**	**200**	**110**	**120**

The following **Table 5** represents features of the AO signatures at 100 mb.

Table 5. AO signature at 100 mb level

	AO pattern by paper [1]	**a) [Our AO] (Fig. 4.4.a)**	**b) [Our AO_1000] (Fig. 4.4.b)**	**c) [Our mean AO] (Fig. 4.4.c)**
Location of **negative** centres	One is displaced slightly off the pole towards Greenland (MAX = -180)	The centre looks like an oval and located over the Arctic Ocean (MAX=-195), over north part of Russia and Alaska, Scandinavian and west Europe to 45ºN latitude	The structure is similar to one of case **b)** at 360 mb **(Fig. 4.3.b)**	The structure is similar to one of case **a)** at 100 mb **(Fig. 4.4.a)**, but the negative centre of action has more dipole structure (one centre is located over Scandinavian and an other is over New Siberian Islands)
MAX, m	**-180**	**-195**	**-113**	**-140**
Location of **positive** centres	There is nearly zonally symmetric positive ring in midlatitudes (MAX = 40 m).	One strong positive center is located over the north-east part of the North America.	The structure is similar to one of case **b)** at 360 mb **(Fig. 4.3.b)**	The structure is similar to one of case **a)** at 100 mb **(Fig. 4.4.a)**
MAX, m	**40**	**190**	**73**	**190**

The comparison of AO structure of paper **[1]** and of case **a)** shows that the main features is that in case **a)** the strongest negative center is displaced from the North pole to Norwegian sea, but its deviation has near the same value. In case **a)** the positive center has stronger deviation comparing to that of [**1**].

The following Table 6 shows features of the AO signatures at 46 mb.

Table 6. AO signature at 50 mb level

	AO pattern by paper [1] at 50 mb	**a) [Our AO] at 46 mb (Fig. 4.5.a)**	**b) [Our AO_1000 at 46 mb] (Fig. 4.5.b)**	**c) [Our mean AO at 46 mb] (Fig. 4.5.c)**
Location of **negative** centres	The structure is similar to AO structure at 100 mb of [**1**].	The same structure as in case **a)** at 100 mb **(Fig. 4.4.a)**	one strong negative center of action is around Beaufort Sea, (MAX = -177) with features around North Atlantic, North Europe to 45ºN latitude (MAX = -60)	The structure similar to case **c)** at 100 mb **(Fig. 4.4.c)** and case **a)** at 46 mb **(Fig. 4.5.a)**
MAX, m	**-270**	**-290**	**-177, -60**	**-255**
Location of **positive** centres	The structure is similar to AO structure at 100 mb of [**1**].	The same structure as in case **a)** at 100 mb **(Fig. 4.4.a)**	There are three positive centers: around the Mediterranean region (MAX=40), around the east part of the USA (MAX = 60), and the wide belt around middle Eurasia and the Pacific Ocean (MAX = 40).	The structure is similar to case **c)** at 100 mb **(Fig. 4.4.c)** and case **a)** at 46 mb **(Fig. 4.5.a)**
MAX, m	**30**	**350**	**60, 40**	**250**

The following **Table 7** demonstrates characteristics of the AO signatures at 30 mb.

Table 7. AO signature at 30 mb level

	AO pattern by paper [1] at 30 mb	**a) [Our AO] at 32 mb (Fig. 4.6.a)**	**b) [Our AO_1000 at 32 mb] (Fig. 4.6.b)**	**c) [Our mean AO at 32 mb] (Fig. 4.6.c)**
Location of **negative** and **positive** centres	The structure is similar to AO structure at 50 mb of [**1**]	The same structure as in case **a)** at 100 mb **(Fig. 4.4.a)**	The structure is similar to one of case **b)** at 46 mb **(Fig. 4.5.b)**	The structure is similar to one of case **c)** at 46 mb **(Fig. 4.5.c)** and one of case **a)** at 32 mb **(Fig. 4.6.a)**
MAX, m	**-365**	**-290**	**-231**	**-330**
MAX, m	**40**	**400**	**57**	**250**

The following **Table 8** illustrates features of the AO signatures at 10 mb.

Table 8. AO signature at 10 mb level

	AO pattern by paper [1]	**a) [Our AO] (Fig. 4.7.a)**	**b) [Our AO_1000] (Fig. 4.7.b)**	**c) [Our mean AO] (Fig. 4.7.c)**
Location of **negative** centres	is centered nearly over the north pole	The same structure as in case **a)** at 32 mb **(Fig. 4.6.a)**	One negative center of action is around the north pole extended to 45ºN around Europe and North America	The structure is similar to one of case **c)** at 32 mb **(Fig. 4.6.c)** and to one of case **a)** at 10 mb **(Fig. 4.7.a)**
MAX, m	**-400**	**-610**	**-373**	**-630**
Location of **positive** centres	is situated over the east part of the Pacific Ocean.	The same structure as in case **a)** at 32 mb **(Fig. 4.6.a)**	are located around the North Atlantic and the east part of the Pacific Ocean	The structure is similar to one of case **c)** at 32 mb **(Fig. 4.6.c)** and to one of case **a)** at 10 mb **(Fig. 4.7.a)**
MAX, m	**100**	**180**	**100**	**190**

The following **Table 9** represents characteristics of the AO signatures at 3.2 mb.

Table 9. AO signature at 3.2 mb level

	AO pattern by paper [1]	**a) [Our AO] (Fig. 4.8.a)**	**b) [Our AO_1000] (Fig. 4.8.b)**	**c) [Our mean AO] (Fig. 4.8.c)**
Location of **negative** centres	No data.	one strong negative centre of action is located over the north pole region up to 45ºN latitude	The structure is close to one of case **b)** at 10 mb (**Fig. 4.7.b**) (MAX=-455) with the feature around the Mediterranean region (MAX = -100)	The structure is similar to case **a)** at 3.2 mb **(Fig. 4.8.a)**
MAX, m		**-1100**	**-455, -100**	**-830**
Location of **positive** centres	No data.	two broad belts are situated: around the North Atlantic and the middle of Eurasia	The structure is close to one of case **a)** at 3.2 mb (**Fig. 4.8.a**)	The structure is similar to case **a)** at 3.2 mb **(Fig. 4.8.a)**
MAX, m		**180**	**148**	**240**

The AO pattern is characterized by geopotential anomalies of the negative sign in the Arctic and anomalies of the positive sign centred about 37°-45ºN. For all obtained AO signatures in cases **a), b), c), d)** one can find these features in some extent. Of course, these AO signatures are not exactly the same as the AO pattern in **[1]** because in our work just only one winter period was taken comparing to 40 years of the paper **[1].**

It is interesting to compare AO indexes and AO structures obtained by several techniques. The mean AO signature in case **c)** (in which AO indexes were calculated for a single field) in the troposphere at 1000 mb, at 460 mb, at 320 mb is close to the AO_1000 signature in case **b)** (in which the regression between AO indexes at 1000 mb and all geopotential anomalies was made). But in the stratosphere at 100 mb, at 46 mb, at 32 mb, at 10 mb, at 3.2 mb the mean AO signature in case **c)** is similar to the AO in case **a)** (in which AO indexes were calculated for each level separately).

As the AO signature at each of 8 levels has been found we can examine how the AO structure propagates from the stratosphere to the troposphere.

Downward propagation of the AO signature. Fig.5

Now we examine the AO signature obtained with the 8-day low pass filter, **Fig. 4.1.d-4.8.d.** The 8 signature maps characterize the AO behaviour at each level, and these signature maps can be compared to the daily anomalies to estimate how close a daily anomaly map is to our pattern representing the AO. If $Z10_{AO}$ is the 10 mb AO signature, and Z10 is a daily map of 10 mb high, then

$\min \left| Z10 - \alpha * Z10_{AO} \right|^2$

defines α as the multiple of $Z10_{AO}$ that results in a "best fit" of the AO signature to the daily map **[1]**.

These calculations were performed for every day of the period December 2002 – February 2003 at each of the 8 levels and we found daily AO coefficients at each level. According to description given

in [**1**] the time series at each level represents the daily value of the AO signature (positive, corresponding to a strong polar vortex (blue in **Fig.5**), or negative, representing a weak vortex (red in **Fig.5**)) and is calculated independently of the other levels. The resulting *AO signature time series* may be used to examine whether AO signals tend to appear at the surface and propagate upward to the stratosphere or vice versa **[1].**
The AO events which correspond to a weak polar vortex can show a remarkable correspondence to stratospheric sudden warmings. The standard definition of warming of World Meteorological Organization requires at 10 mb easterly winds at 60ºN latitude and warmer temperatures at the pole than at 60ºN latitude. In the frames of this work we examine the temperatures field only and do not consider wind data.

Fig.6 represents the temperature around the North Pole (red) and mean zonal temperature at 60ºN latitude (blue) at 10 mb. We can see that the temperature at the pole was higher than at 60ºN latitude around **28 December 2002 – 8 January 2003; 13-22, 24-28 January; 1-6, 12-28 February**. The highest temperature at the pole was observed around 31 December, 18 and 27 January.
Meanwhile **Fig.5** shows a weak polar vortex (red) around **17-27 January 2003** between layers of **10 – 1000 mb** and around **15-25 February 2003** between **10-100 mb** layers. **Fig.5** and **Fig.6** demonstrate near same conditions when there was a stratospheric warming and a weak polar vortex.
Unfortunately certainly cannot say that in **Fig.5** we have a clear downward propagation from the stratosphere to the troposphere in a few weeks as it was described in [**1**]. To quote from [**1**], "Many of the stratospheric events are connected to tropospheric events, but the connection is typically intermitten, involving fairly rapid bursts which tend to descend farther into troposphere over period of several weeks. Some stratospheric events do not reach the troposphere. Typically, the AO anomalies begin at 10 mb or above and move downward of few weeks**."**
In our case, the winter 2002/2003 there is no evidence for such behaviour. Rather, bursts are simultaneous at all heights, or appear first at 1000 mb and propagate upwards.

PART 2

Correlation maps between the temperature at Abisko-station at 1000 mb and the temperature at other levels around the North Hemisphere

The 8-day low pass filter was chosen based on a preliminary Fourier transformation which revealed an 8-day harmonic in the frequency spectrum of temperature at Abisko station at 1000 mb during the period of December 2002 – February 2003. The 8 day filtering procedure was applied to the temperature at all levels around the North Hemisphere. Then a cross-correlation analysis using a lag interval [-60,60] days was performed for the temperature data at Abisko-station and each other level. We have looked for lags with maximal correlation coefficients. **Table 10** summarizes lags and correlation coefficients which are more than 0.5.

Table 10

level	lag days	R max with the 95% confidence interval.	Figure
3.2 mb	54	0.55<**0.68**<0.78	
	53	0.56< **0.69**<0.78	
	52	0.56< **0.69**<0.78	**Fig.7.8.1,** (0.69*0.69=0.48), 48%
	51	0.56< **0.69**<0.78	
	50	0.37 <**0.54**<0.67	
	22	0.46<**0.61**<0.72	
	21	0.47 <**0.62**<0.73	**Fig.7.8.2**
	20	0.45<**0.60**<0.72	
10 mb	**52**	0.47<**0.62**<0.73	**Fig.7.7.1**
	51	0.42<**0.58**<0.70	
	50	0.37<**0.54**<0.67	
	20	0.68<**0.78**<0.85	**Fig.7.7.2,** (0.78*0.78=0.61), 61%
	19	0.68<**0.78**<0.85	
	18	0.66<**0.76**<0.84	
32 mb	**19**	0.68<**0.78**<0.85	**Fig.7.6,**(0.78*0.78=0.61), 61%
	18	0.66<**0.76**<0.84	
	16	0.52<**0.66**<0.76	
46 mb	**19**	0.64<**0.75**<0.83	**Fig.7.5,** (0.75*0.75=0.56), 56%
	18	0.62<**0.73**<0.81	
	16	0.49<**0.63**<0.74	
	12	0.49<**0.63**<0.74	
100 mb	**19**	0.60<**0.72**<0.81	**Fig.7.4,** (0.72*0.72=0.52), 52%
	16	0.60<**0.72**<0.81	
	14	0.60<**0.72**<0.81	
	12	0.51<**0.65**<0.75	

Fig.7.8.1 and **Fig.7.7.1** show the similar structures with lag of **52 days back** at **3.2 mb** and at **10 mb**. There is a correlation field with the positive correlation (R= 0.6 - 0.65) around the North Atlantic Ocean, the North Europe, Scandinavian and the north pole with features around Kamchatka and the west-north part of the Pacific Ocean.
From these figures one can see that the maximal correlation coefficient reaches to 0.69 with **lag of 52 days back** (at 3.2 mb and at 10 mb). This means that only 48% (0.69*0.69=0.48) of temperature variability at Abisko (at 1000 mb) can be statistically explained by the temperature changes at the region around the North Atlantic Ocean, the North Europe, Scandinavia and the north pole at **3.2-10 mb**.
Fig. 7.7.2, 7.6, 7.5 and **7.4** demonstrate similar structures with lag of **19-20 days back** at **10 mb,** at **32 mb,** at **46 mb** and at **100 mb.** One can see **one** center with positive correlation (R = 0.72 – 0.78) around the North Atlantic Ocean, the North Europe and Scandinavian. It looks like a positive correlation field between **10 – 100 mb**.
From these figures it follows that the maximal correlation coefficient reaches 0.72-0.78 with a **lag of 19-20 days back** (at 10-100 mb). This means that 52-61% of the temperature variability at Abisko (at 1000 mb) may be statistically explained by the temperature changes at the region around the North Atlantic Ocean, the North Europe and Scandinavia at **10-100 mb**.

The statistical predictability of temperature variability at Abisko (48% and 52-61%) is not particularly good. But we found no better correlation fields with lags outside these ranges (52 and 19-20 days back) than those shown in **Fig.7.8.1, Fig.7.7.1** and in **Fig. 7.7.2, 7.6, 7.5, 7.4.**

The statistical results for the **320 mb**, **460 mb** and **1000 mb** levels are listed in **Table 11.**
Table 11.

level	lag days	R max with the 95% confidence interval.	Figure
320 mb	7	0.70<**0.79**<0.86	
	5	0.79< **0.86**<0.90	**Fig.7.3** (0.86*0.86=0.7396), 74%
	4	0.78< **0.85**<0.90	
460 mb	4	0.77 <**0.84**<0.89	
	3	0.81<**0.87**<0.91	**Fig.7.2** (0.87*0.87=0.7569), 76%
	2	0.79< **0.86**<0.90	
	1	0.75<**0.83**<0.88	
1000 mb	**0**	0.91<**0.94**<0.96	**Fig.7.1** (0.94*0.94=0.8836), 88%

Table 11 shows good correlation coefficients on the whole between the temperature at Abisko and the temperature around the North Hemisphere at 320-460 mb.
Fig.7.3-7.1 demonstrate that a **few small centres** with positive correlation coefficient are located around the Arctic Ocean, Scandinavia, around the north part of Africa and east part of the Atlantic Ocean. Also **Fig.7.3-7.1** illustrate a **few small centres** with negative correlation coefficient around the Mediterranean region, Indian and the north part of the Atlantic Ocean.
We can not certainly say that the correlation structure at 100 mb of only one positive correlation center with lag of 19 days back (**Fig.7.4**) propagates directly to 320 mb (with a lag of 5 days back (**Fig.7.3**)) where **a few centres** of positive correlation appear instead of **one** positive centre .

So we find that temperature variability at Abisko (at 1000 mb) can be statistically explained to some extent (about 48% and 52-61%) by the temperature changes at **3.2-10 mb** with lag of **52 days back**

and **at 10-100 mb** with lag of **19 days back**. The 10 mb level was taken two times into consideration using two different lags and two different correlation fields.

Looking in more detail, we consider **16 February 2003** (when the maximal temperature during the winter period at Abisko took place, T = 277.15 K) . The temperature data were analyzed at 3.2 mb **(Fig.8.8)** and at 10 mb **(Fig.8.7.1)** on **26 December** 2002 (**52 days back** from 16 February), and on **28 January** 2003 (using **19 days back** from 16 February) at 10 mb **(Fig.8.7.2),** at 32 mb (**Fig.8.6**), at 46 mb **(Fig.8.5)** and at 100 mb **(Fig.8.4) .**

Fig.8.8 (on **26 December**) demonstrates that high temperature centre (**280-300 K)** is situated around the Arctic Ocean and the North Europe and cold centre (**200-220 K)** is located around the North Pole with a shift to Alaska and to 50˚N latitude at **3.2 mb**. The similar pattern with temperature in centres **240-260 K** and **180-210 K** respectively are situated at **10 mb (Fig.8.7.1).** The warm temperature centres represents a stratospheric warming at 3.2-10 mb levels.

The stratospheric warming is illustrated in **Fig.2** where one can see the fast growing temperature on **25-27 December** at 10 mb and at 3.2 mb. At the same time **Fig. 3** shows us the stratospheric warming during **25 December 2002 – 5 January 2003** at 3.2-10 mb as well. One can suppose that this warming started earlier than 25 December and at higher altitudes. But in frames of this work we do not take into account higher levels than 3.2 mb.

Fig.8.6-8.4 on 28 January show **two** warm centres with the same temperature (225-230 K) at 32-100 mb that are located opposite to each other (first is around the North Europe and second is around Alaska-Kamchatka region). At the same time **Fig.8.7.2** on **28 January** at 10 mb demonstrates **only one** warm centre with T=237 K located around the North Atlantic and the North Europe. It means that 10 mb and 32 mb levels have different temperature structures simultaneously.

Fig.1-3 and **Fig.6** illustrate that the stratospheric warming was observed at 10-100 mb above Abisko area during **25-30 January 2003.** Probably this stratospheric warming started earlier than 25 January and at higher altitudes.

So we have considered two periods (**25 Dec. 2002 – 5 Jan. 2003** and **25-30 Jan. 2003**) when stratospheric warmings took place. **26 December** (52 days back from the warmest winter day in Kiruna (16.02.03)) and **28 January** (19 days back) are contained just inside of these periods**.**

Discussion and conclusion

The task of this work was to attempt to find the cause of the unusual warm weather in Kiruna in winter season 2002-2003. Two main ideas were proposed to solve this task. First idea was to research the effect of the Arctic Oscillation and the second one was to check the correlation connection between weather conditions in Abisko-station at 1000 mb and dynamic processes at 460 - 3.2 mb in the North Hemisphere.

In the first case geopotential data were taken into consideration, whereas the temperature field was analyzed in the second case. The resulting AO pattern in our work is somewhat different from general AO pattern found in the paper [**1**]. The main reason is that **40 years** data (90-day low pass filtered) were used in general pattern while **one winter period 2002-2003** (8-day low pass filtered) was only considered in our case study. So our AO pattern may be considered as a particular structure of the general AO pattern.

Examining our AO time series (**Fig.5**) it is difficult to observe clear downward propagation in a **few weeks** from the stratosphere to the troposphere as one can find in [**1**]. This may be explained by two reasons. The first one is the statistical effect: in our work a very short sample was analyzed (3 month

only) while 40 years data set were examined in the paper [**1**] and therefore one can expect another AO time series represented an isolated case of primary AO time series [**1**]. An other reason is physical: probably the downward stratospheric warming did not propagate from the stratosphere to the troposphere in a few weeks in this winter period. Sometimes the stratospheric events do not reach the lower troposphere as mentioned in paper [**2**].

It was found in the paper [1] that in several cases the stratospheric warming propagated to the lower troposphere in a few weeks. In our work we have found the stratospheric warming around **17-27 January 2003** between layers of **10 – 1000 mb** and around **15-25 February 2003** between **10-100 mb** layers but they have no clear phase–time shifts in the stratosphere-troposphere system. Therefore it is difficult to conclude in which direction did the analyzed warmings go. Meanwhile the authors of paper [**1**] note that AO signals tend to appear at surface and **propagate upward to the stratosphere or vice versa**. And in fact one can find the confirmation to these words looking at **Plate 2 [1]** where AO signals move in different directions in the lower troposphere-stratosphere system.

The cross-correlation analysis shows that temperature variability at Abisko (at 1000 mb) can be statistically explained in some extent by the temperature changes at **3.2-10 mb** (by 48%) with lag of **52 days back** and at **10-100 mb** with lag of **19 days back** (52-61%). Perhaps the stratospheric warming observed at 3.2 mb-10 mb propagated to layers of 10 mb -100 mb in about **one month** and then proceeded to move to 1000 mb in about **19-20 days**. It is not possible to say exactly what happened with this stratospheric warming when it reached 100 mb level and which way this warming propagated to the low troposphere .
It is notable in **Figure 8** that the spatial patterns of temperature variations have the characteristics of planetary waves with wave number 1 at 10 mb and above and wave number 2 between 100 mb and 10 mb. This suggests it may be useful to analyse the data in terms of planetary-waves rather than EOFs.

References

1. Baldwin, M.P., and T.J. Dunkerton, Propagation of the Arctic Oscillation from the stratosphere to the troposphere, *J. Geophys. Res*., *104*, D24, 30.937-30.946, 1999.
2. Baldwin, M.P., The Arctic Oscillation and its role in stratosphere-troposphere coupling, *Sparc,* N. 14, pp. 10-14, 2000.
3. Thompson, D.W.J., and J.M. Wallace, The Arctic Oscillation signature in the wintertime geopotential heights and temperature fields, *Geophys. Res. Lett., 25*, 1297-1300, 1998.
4. Wilks, D. S., Statistical Methods in the Atmospheric Sciences, *V. 59 in International Geophysics series,* 1995.

Fig.1

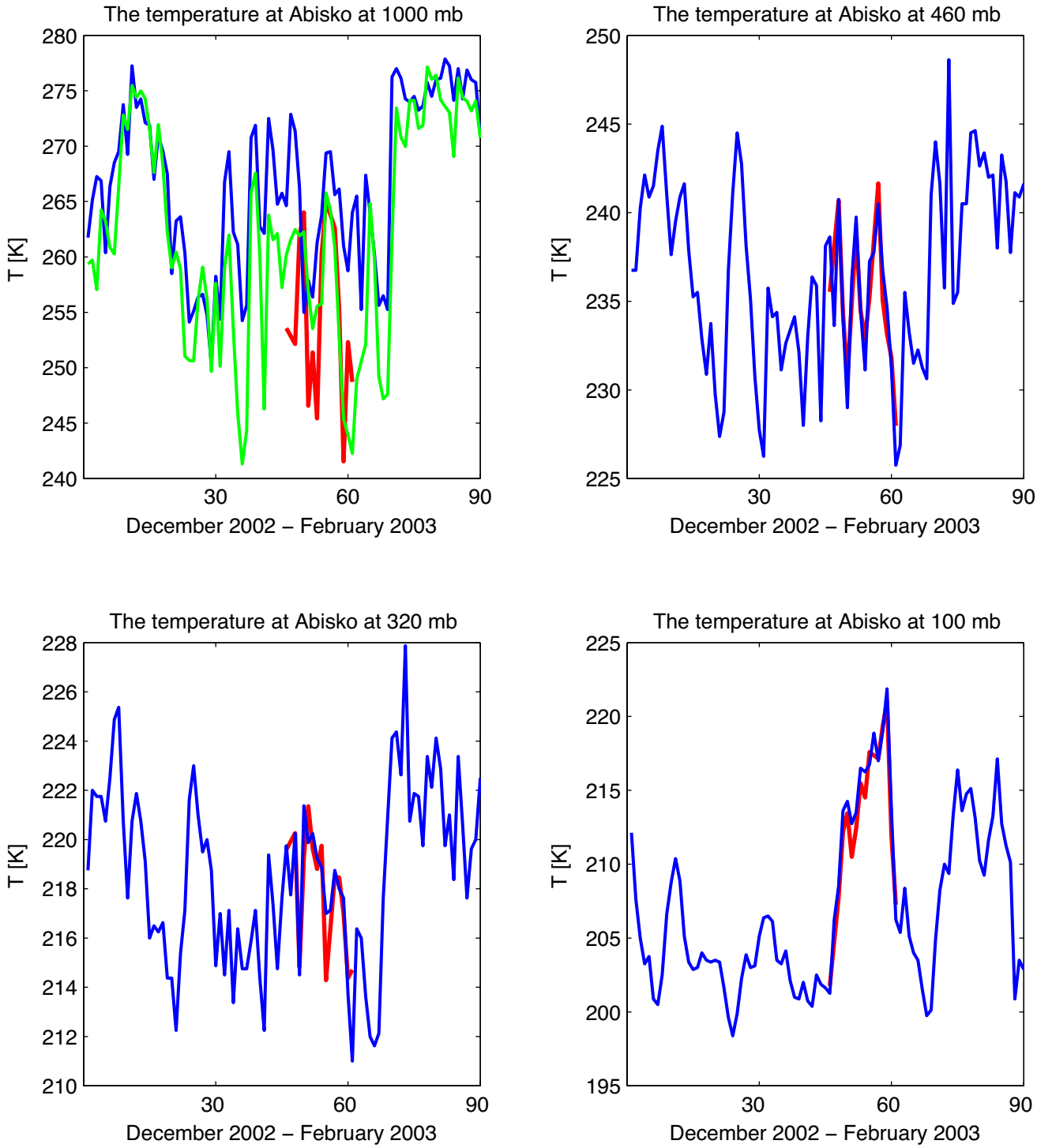

Green line is Abisko–station data (68N21, 18E49), blue line – UKMO data at the point (67N30, 18N45), red line – radiosonde/rocket data from Esrage (67N53, 21E06)

Fig.2

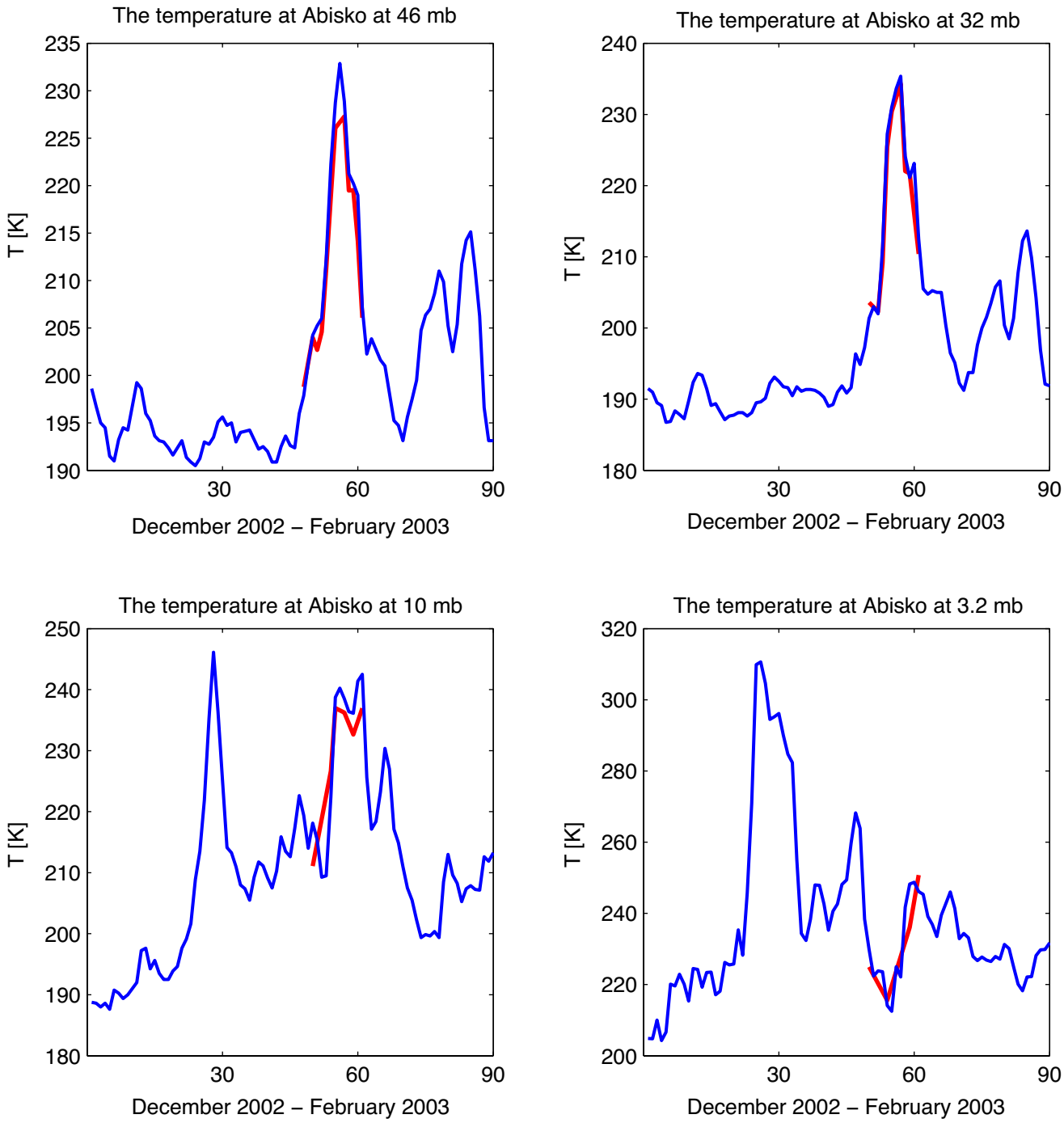

Blue line – UKMO point (67N30, 18N45), red line – radiosonde/rocket data from Esrage (67N53, 21E06)

Fig.6 (10 mb level. Red – temp. around the north pole, blue – mean zonal temp. at 60N latitude)

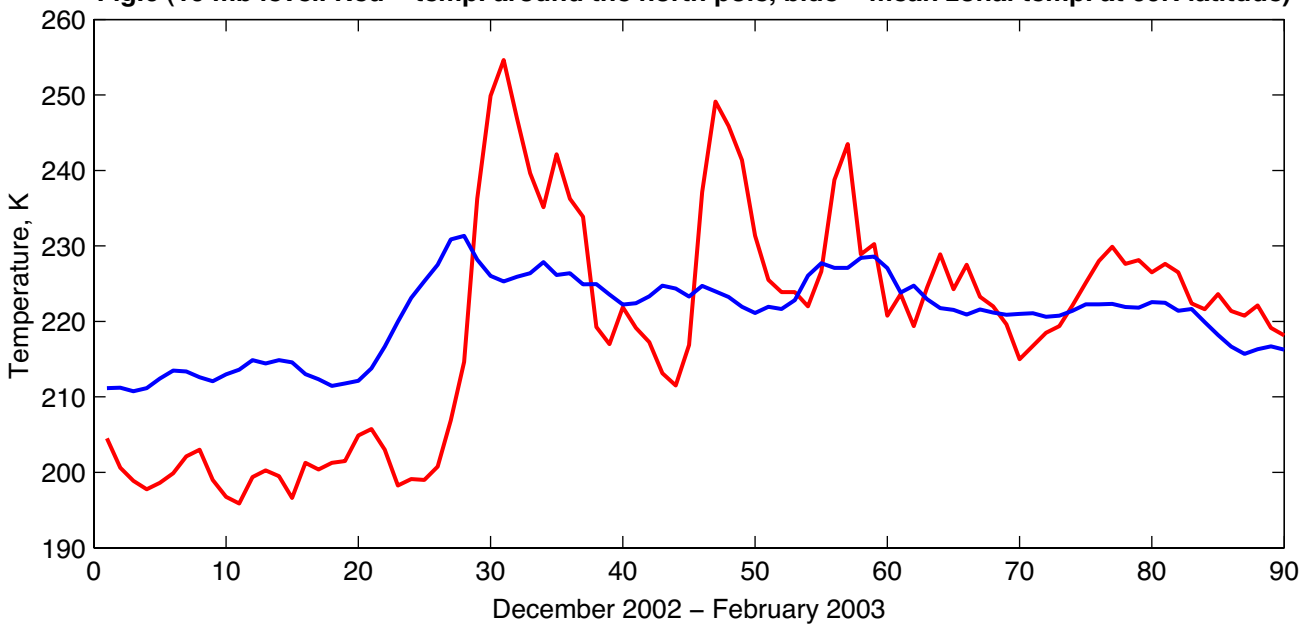

Fig.3 (The temperature around Abisko at 1000 – 3.2 mb)

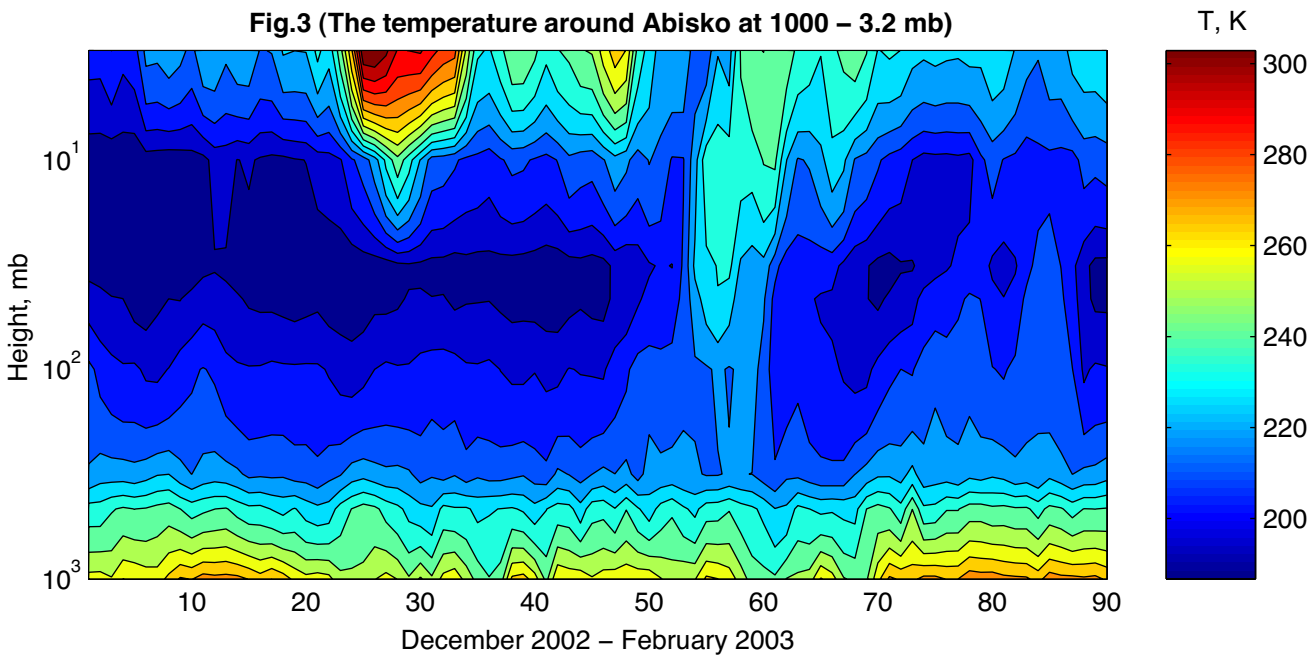

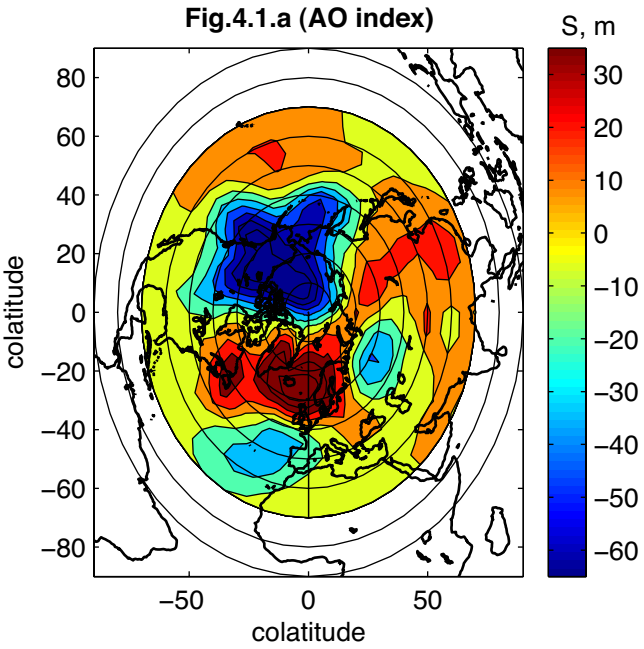

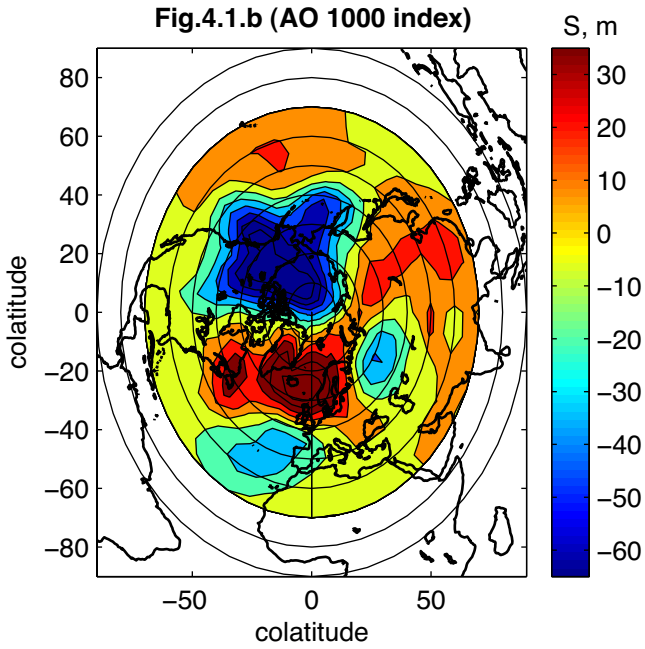

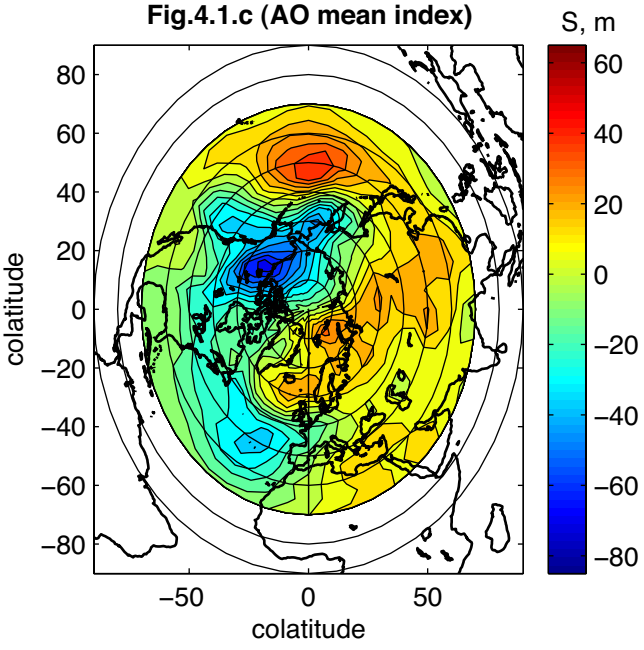

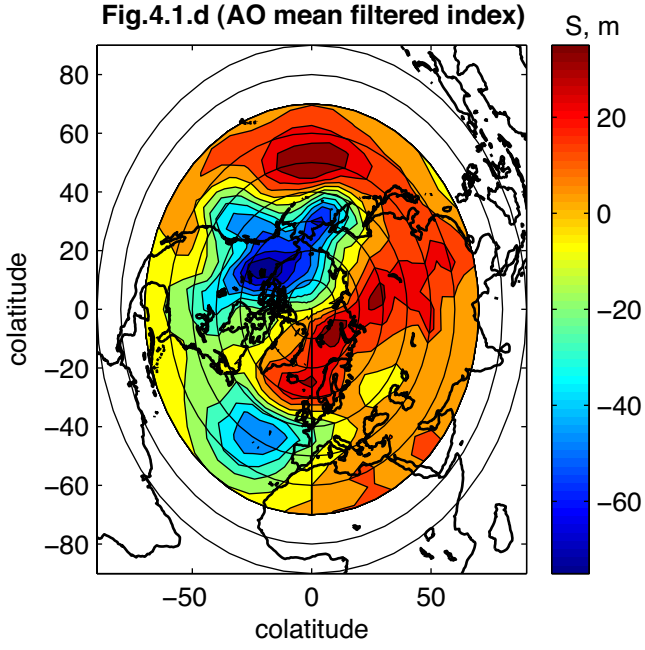

Spatial signatures of the AO at 1000 mb produced by regressing the AO index with geopotential. Contour values are meters, corresponding to a one standard deviation anomaly (S) in the AO index. December 2002 – February 2003.

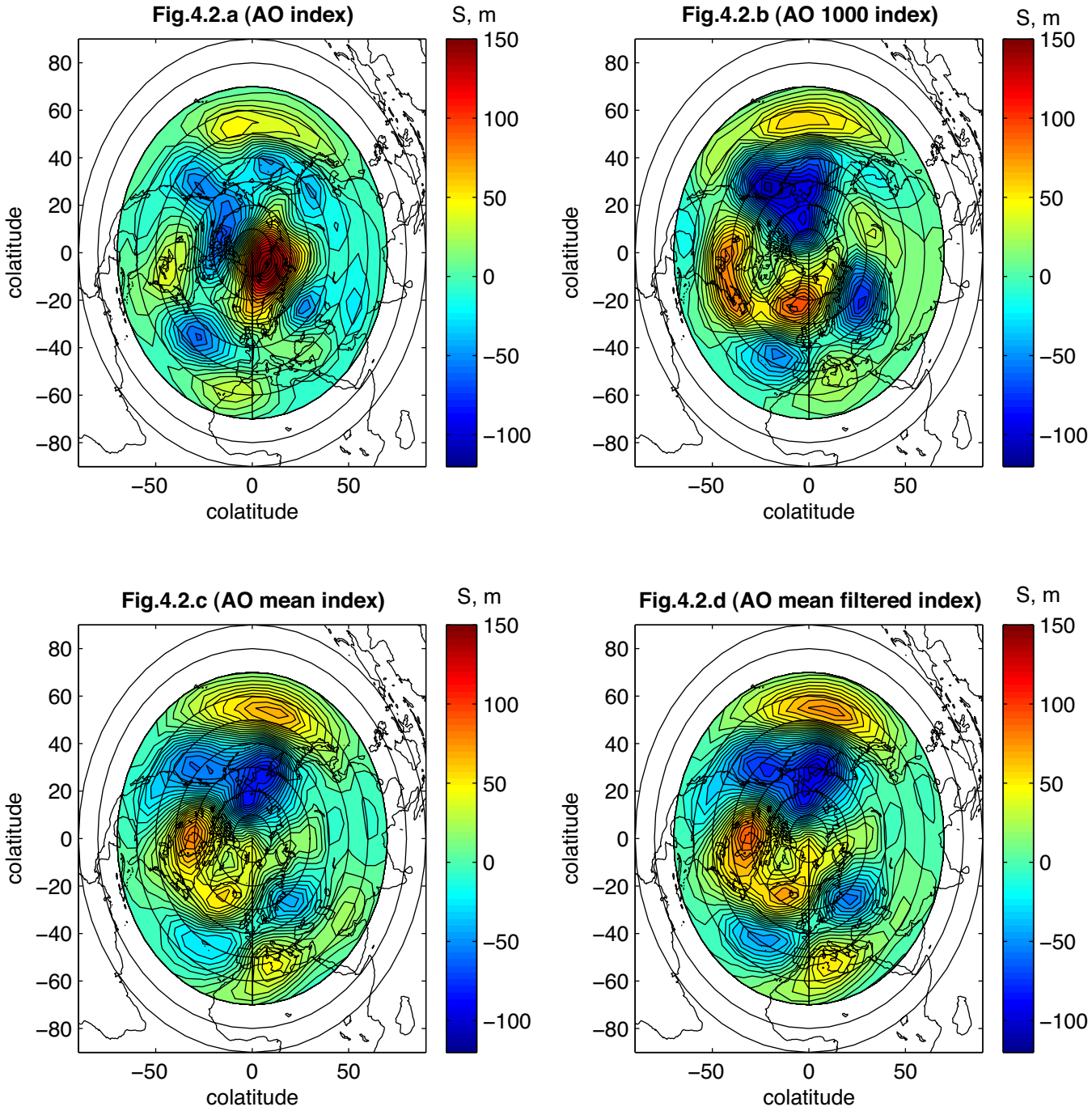

Spatial signatures of the AO at 460 mb produced by regressing the AO index with geopotential. Contour values are meters, corresponding to a one standard deviation anomaly (S) in the AO index. December 2002 – February 2003.

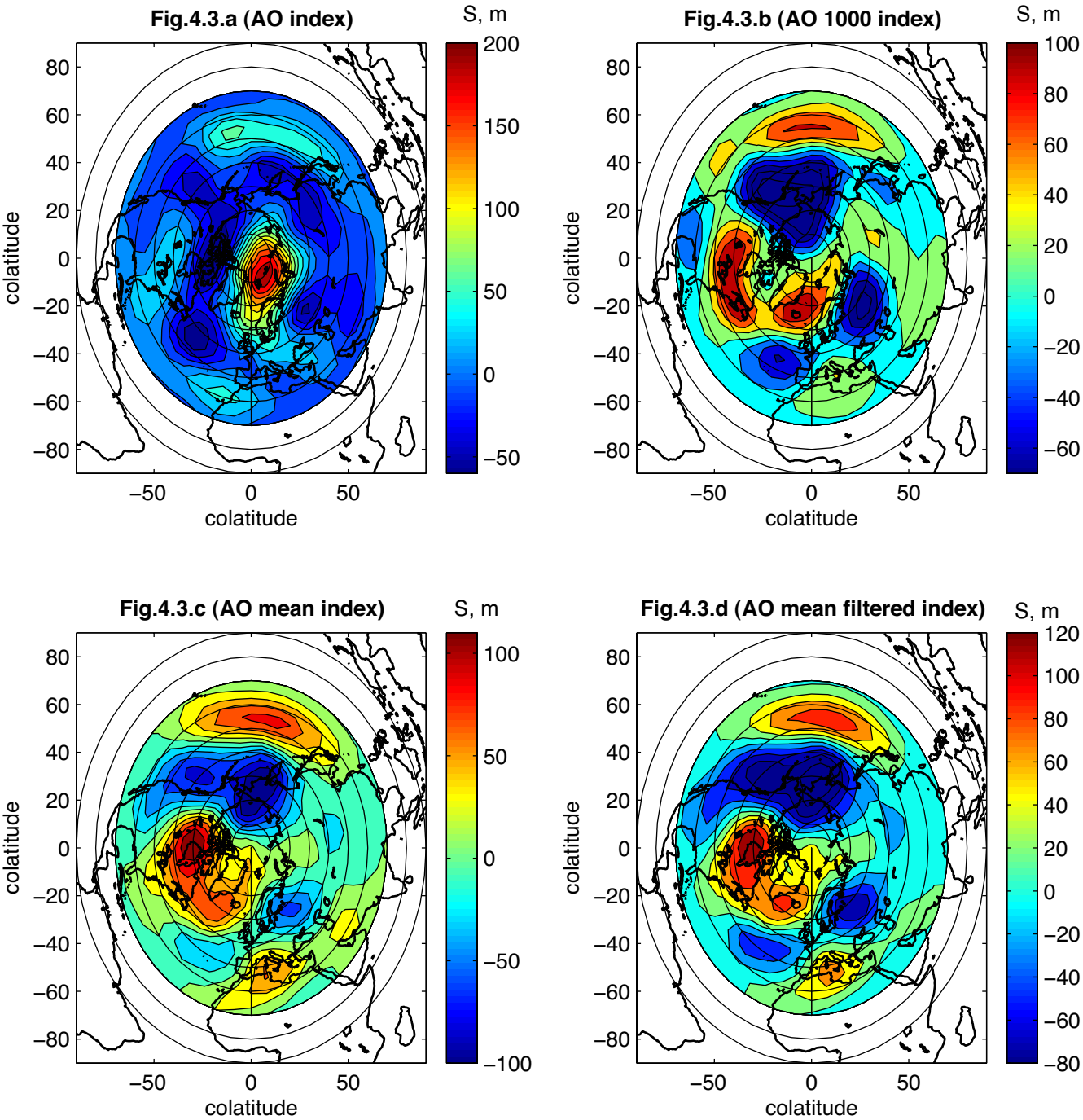

Spatial signatures of the AO at 320 mb produced by regressing the AO index with geopotential. Contour values are meters, corresponding to a one standard deviation anomaly (S) in the AO index. December 2002 – February 2003.

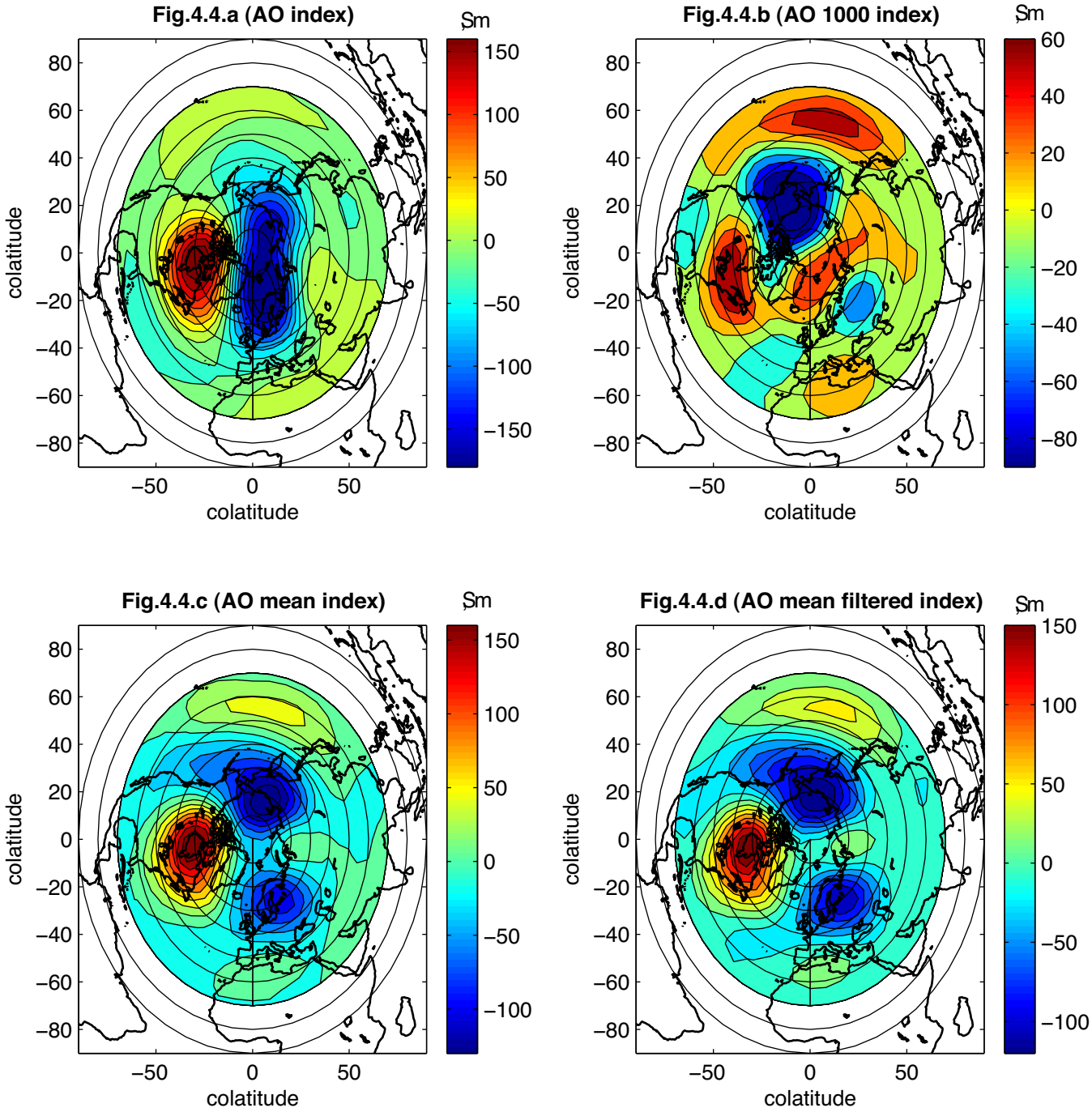

Spatial signatures of the AO at 100 mb produced by regressing the AO index with geopotential. Contour values are meters, corresponding to a one standard deviation anomaly in the AO index. December 2002 – February 2003.

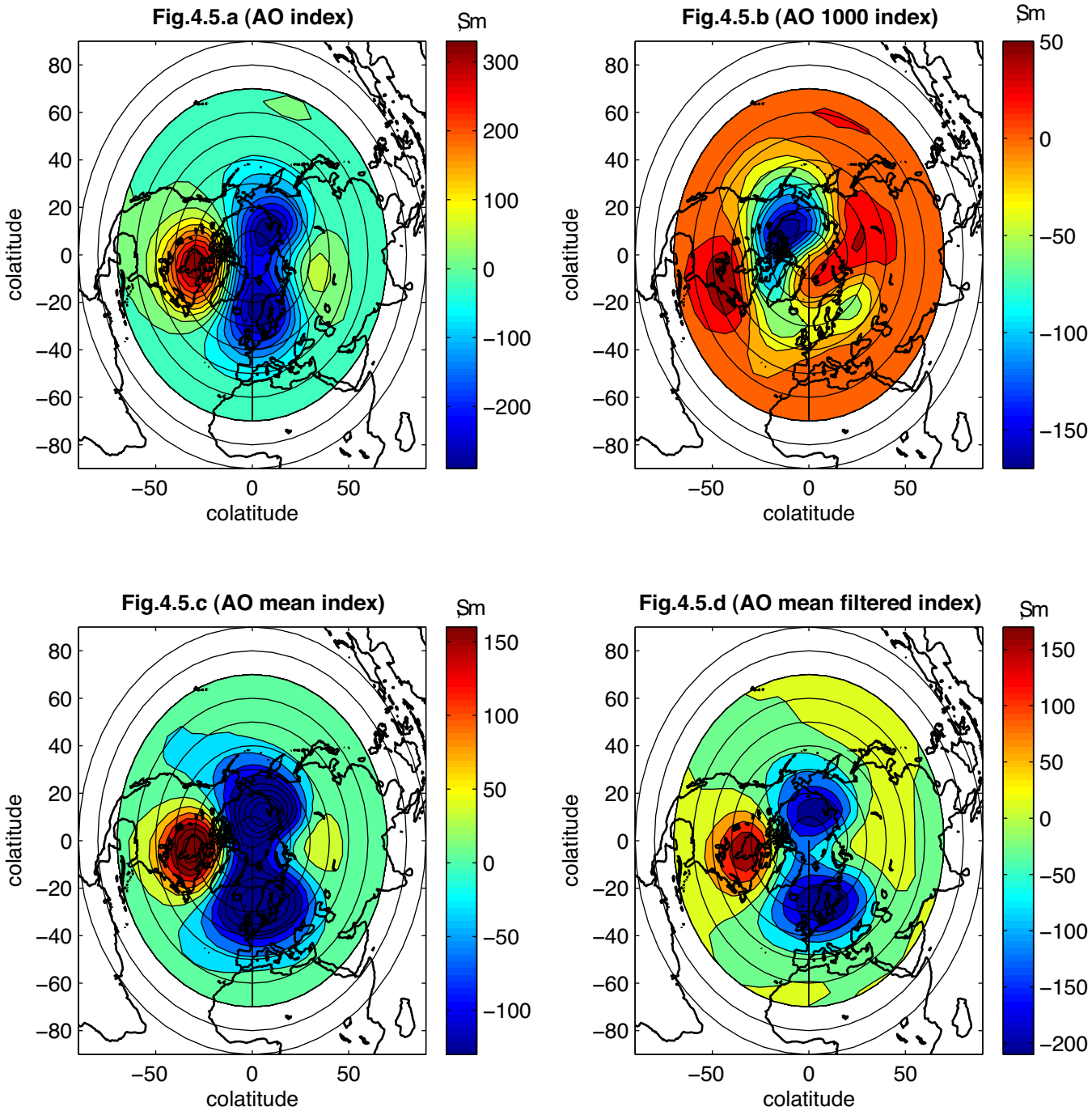

Spatial signatures of the AO at 46 mb produced by regressing the AO index with geopotential. Contour values are meters, corresponding to a one standard deviation anomaly in the AO index. December 2002 – February 2003.

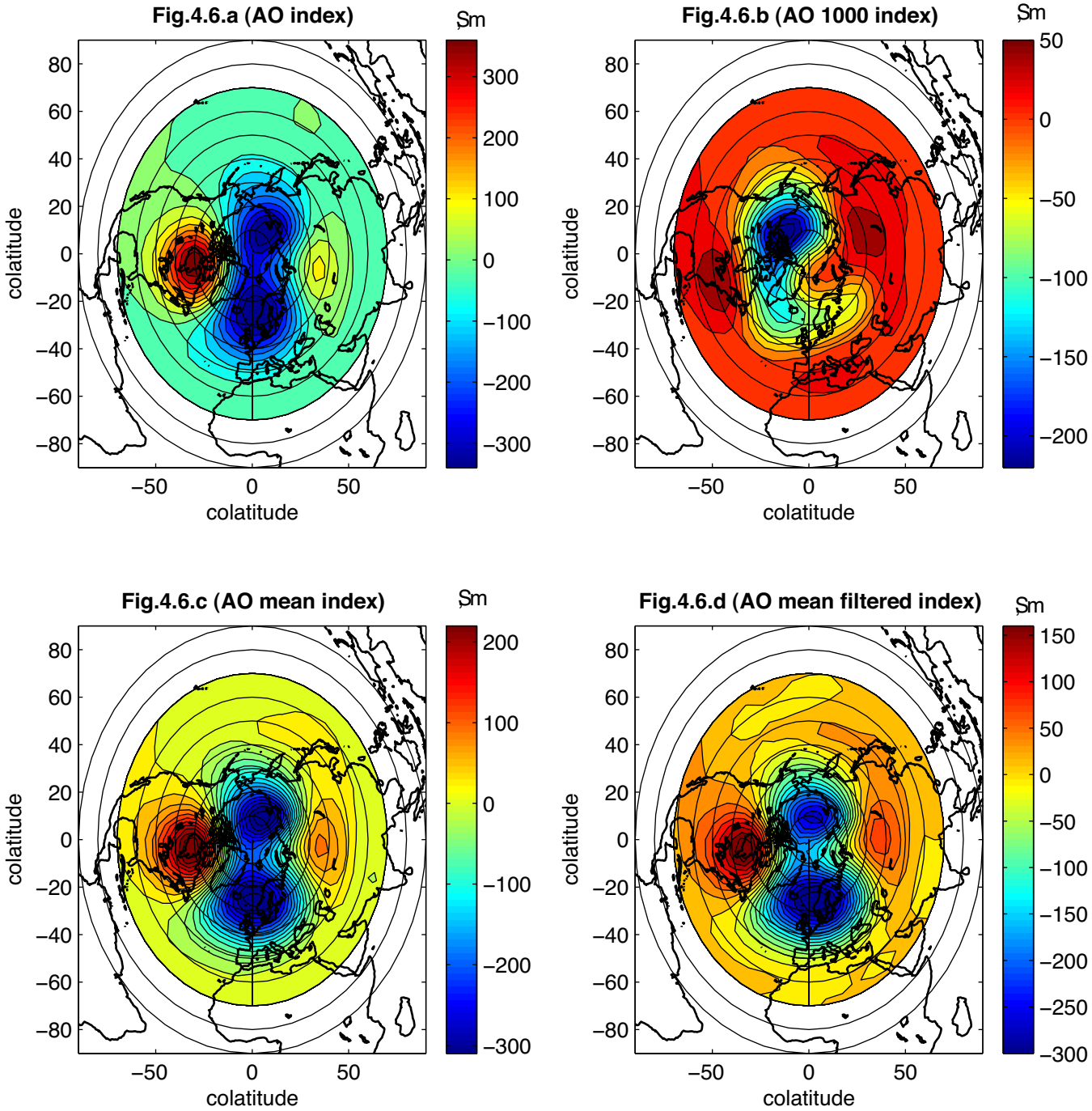

Spatial signatures of the AO at 32 mb produced by regressing the AO index with geopotential. Contour values are meters, corresponding to a one standard deviation anomaly in the AO index. December 2002 – February 2003.

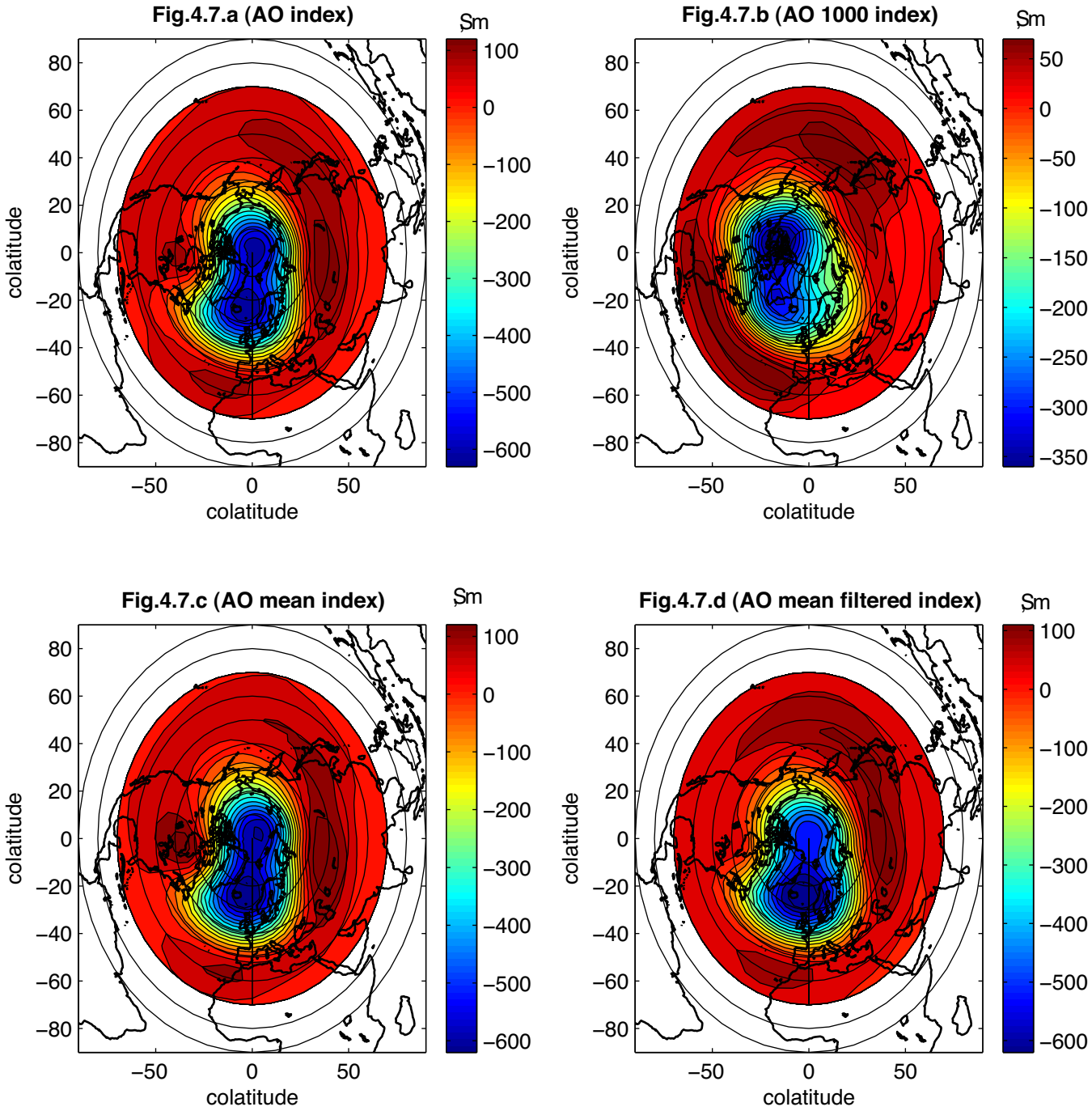

Spatial signatures of the AO at 10 mb produced by regressing the AO index with geopotential. Contour values are meters, corresponding to a one standard deviation anomaly in the AO index. December 2002 – February 2003.

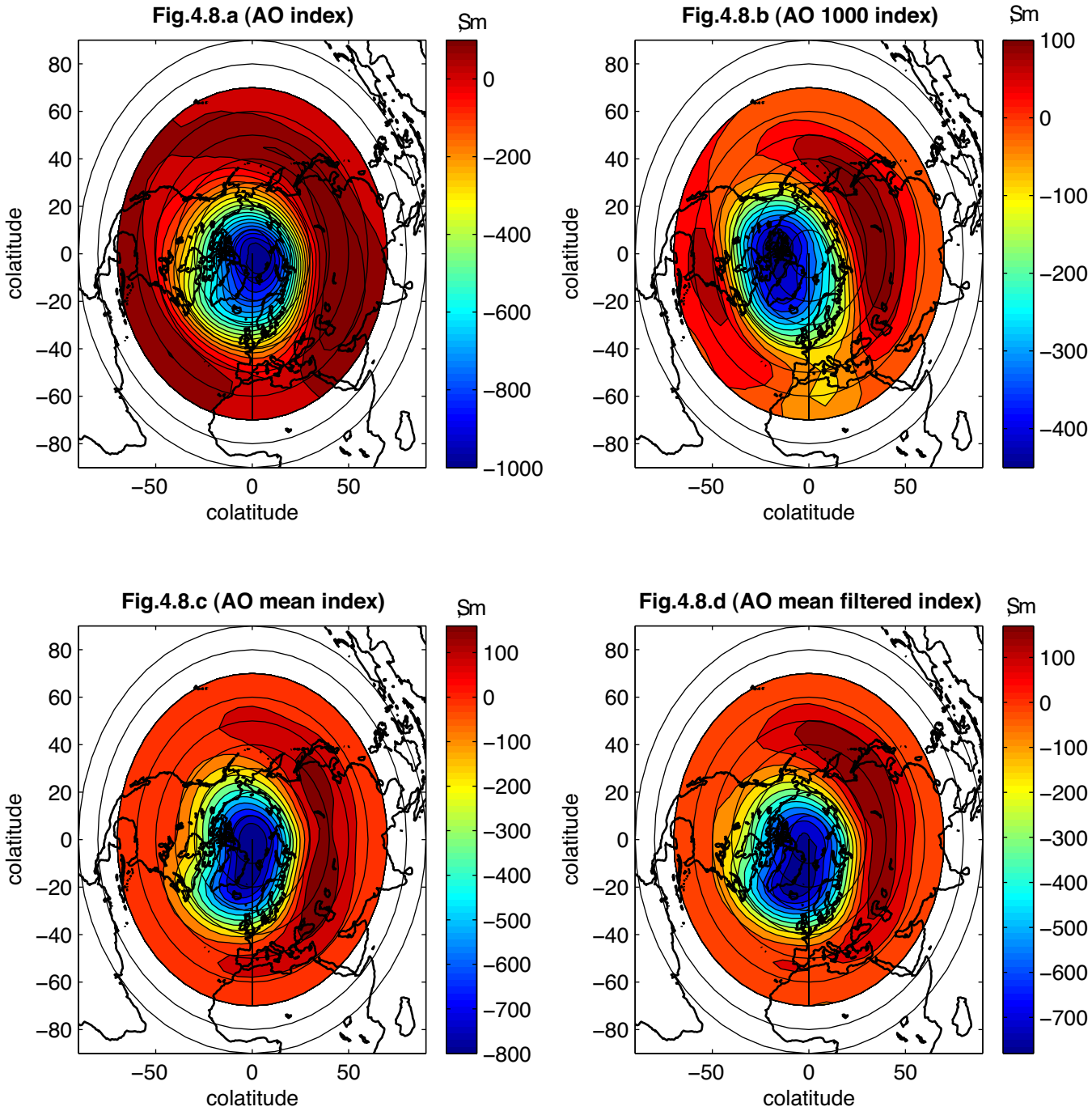

Spatial signatures of the AO at 3.2 mb produced by regressing the AO index with geopotential. Contour values are meters, corresponding to a one standard deviation anomaly in the AO index. December 2002 – February 2003.

Fig. 5 Mean AO signature time series based on 8–days low–pass filtred geopotential height .
Period is December 2002 – February 2003. Contours are +/+3.0, +/–2.0, +/–1.5, +/–1, +/–0.5.
Red corresponds to a weak, varm polar vortex, while blue indicates a strong, cold vortex.

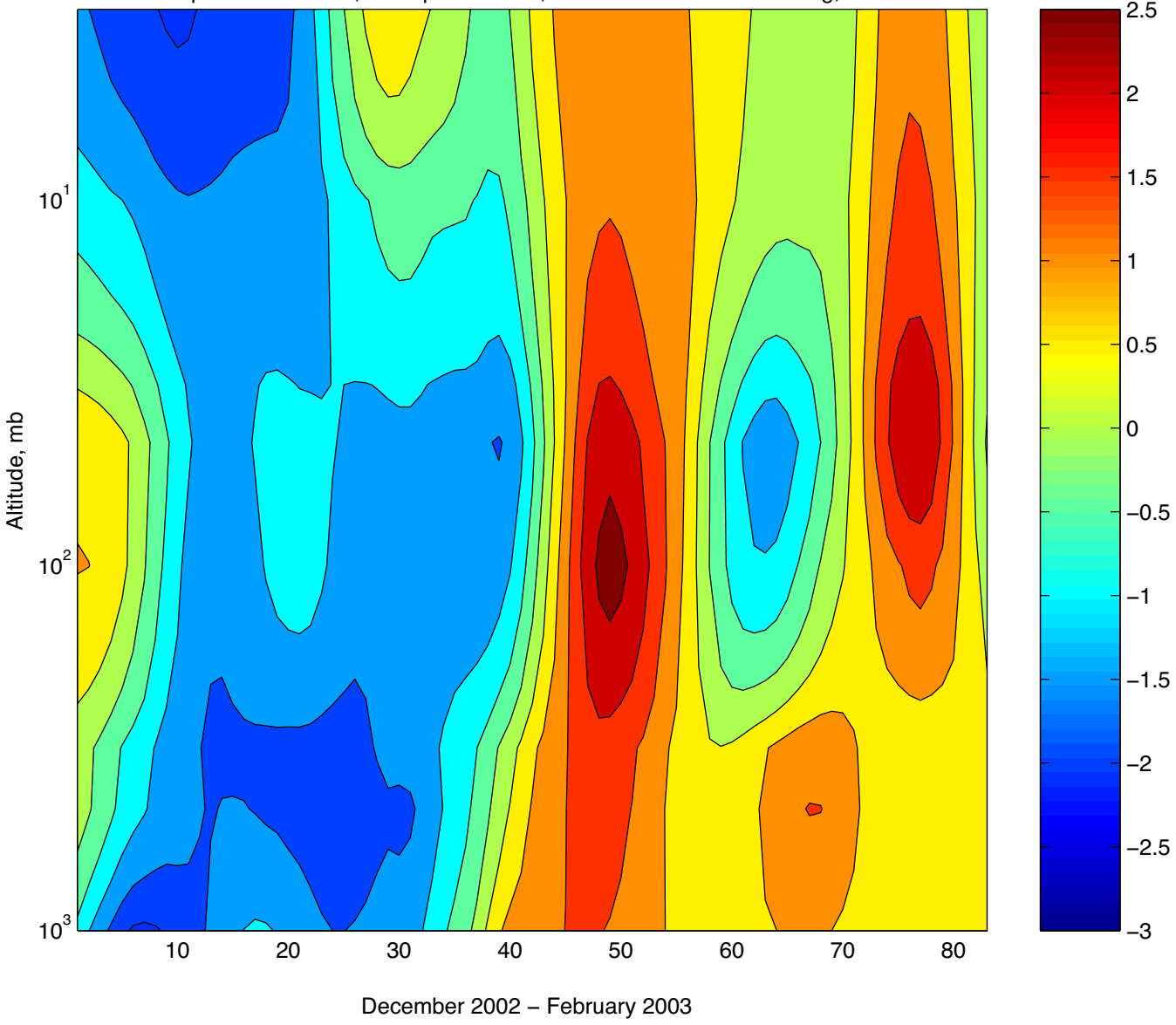

Fig.6 (10 mb level. Red – temp. around the north pole, blue – mean zonal temp. at 60N latitude)

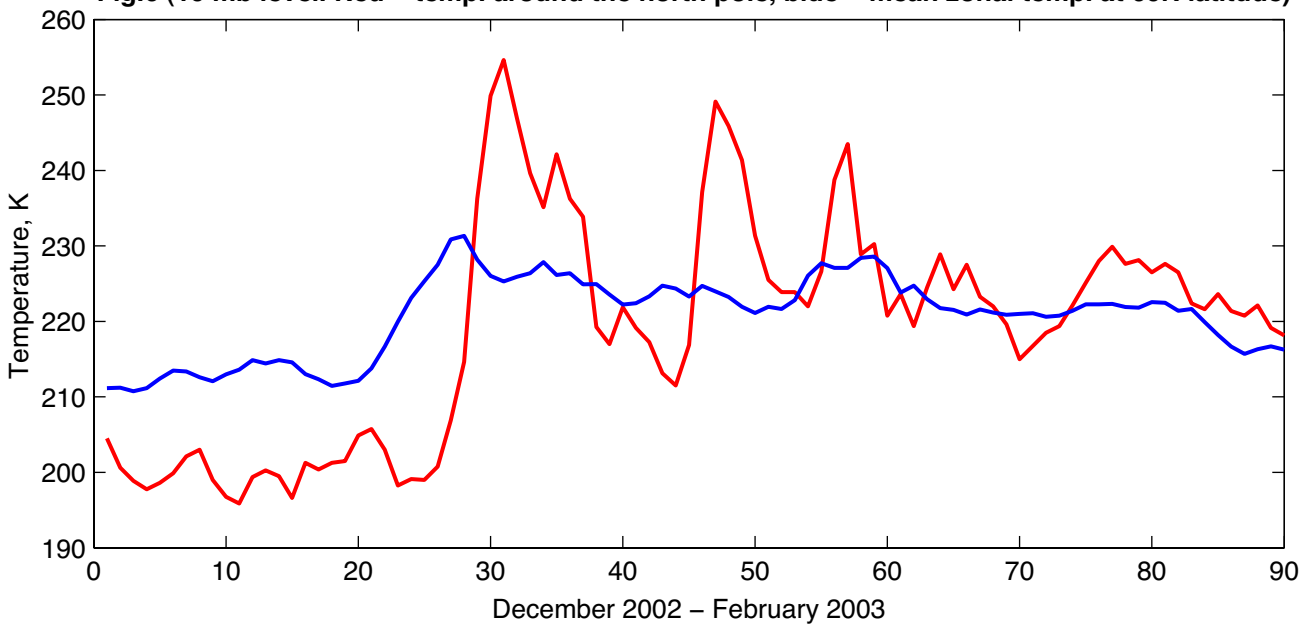

Fig.3 (The temperature around Abisko at 1000 – 3.2 mb)

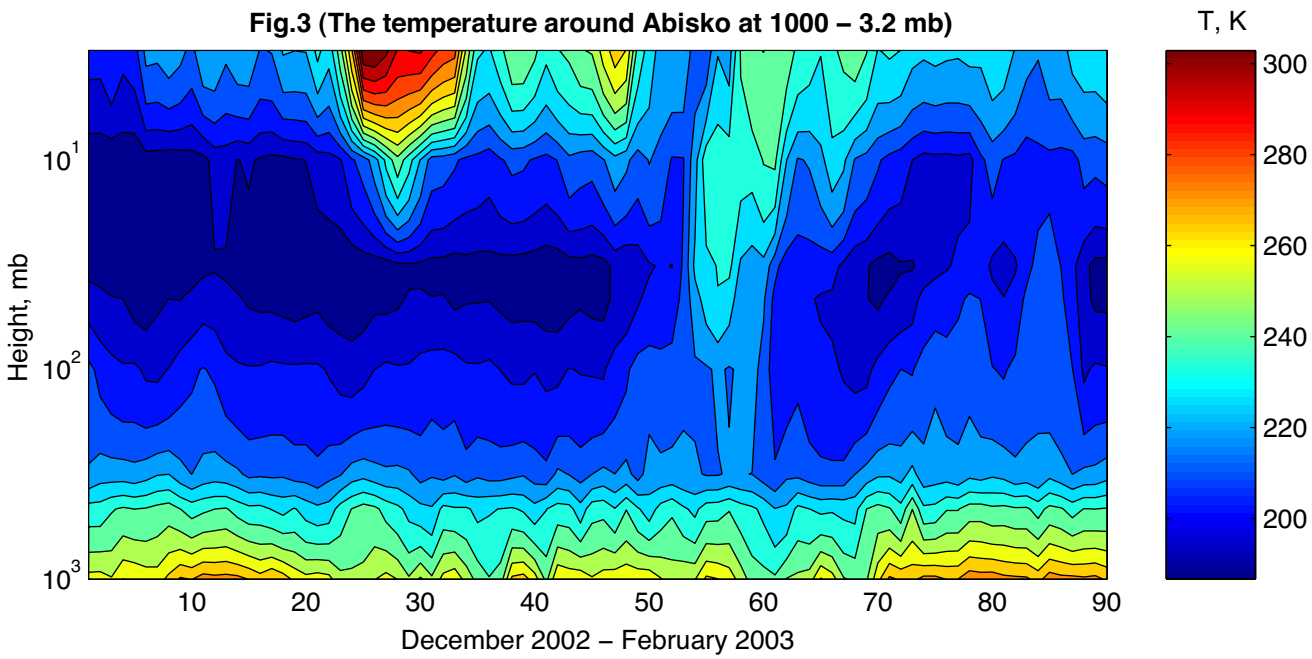

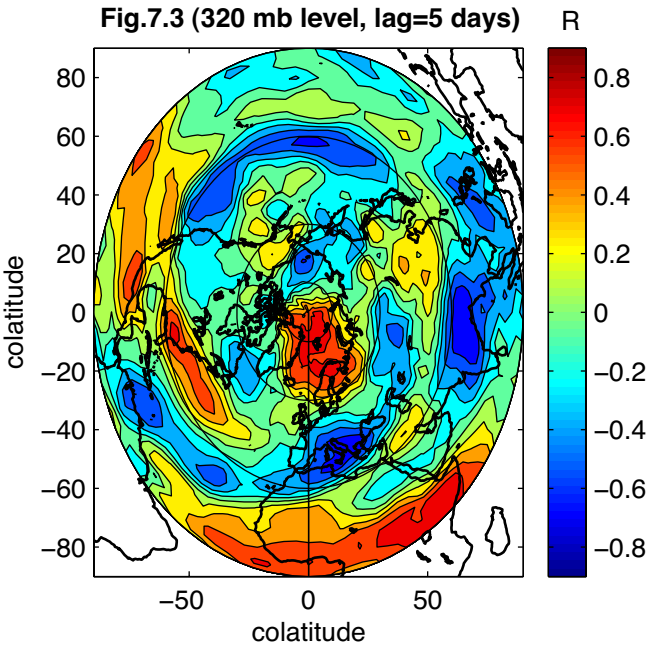

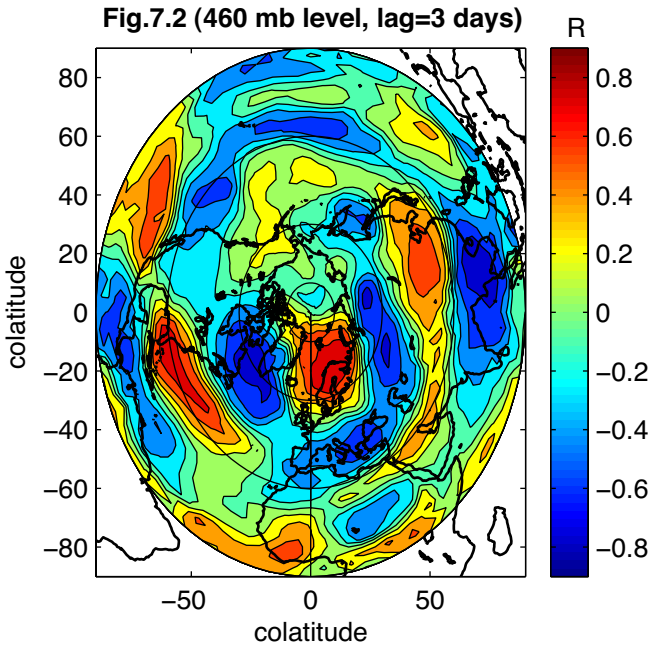

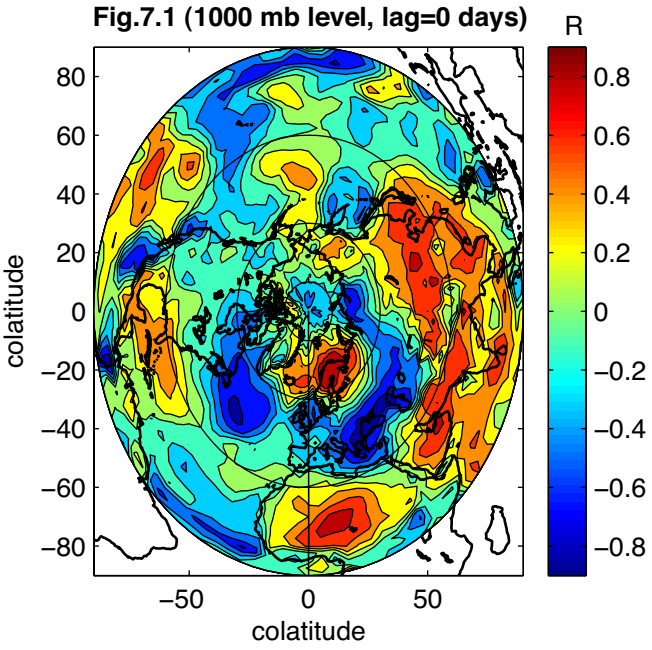

Correlation maps of the 8−day low−pass filtered temperature data at location around the North Hemisph. at 320−1000 mb and with that at Abisko at 1000 mb with lag of 0−5 days back for the period December 2002 − February 2003.

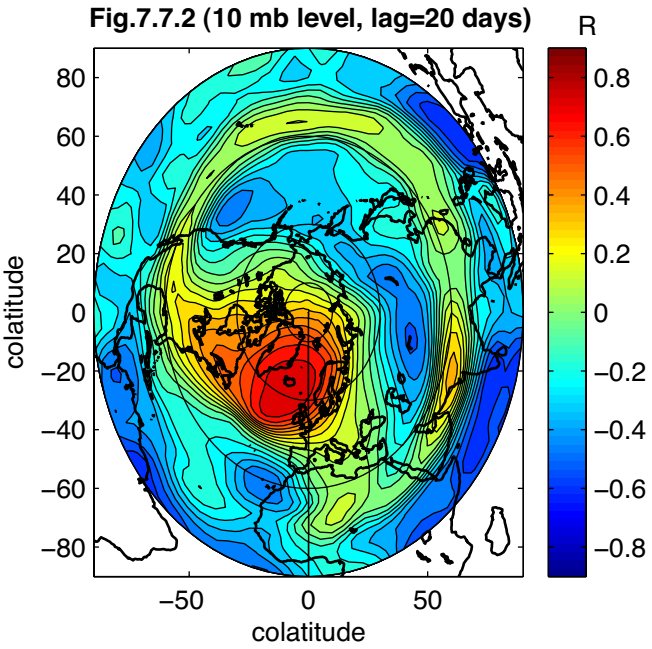

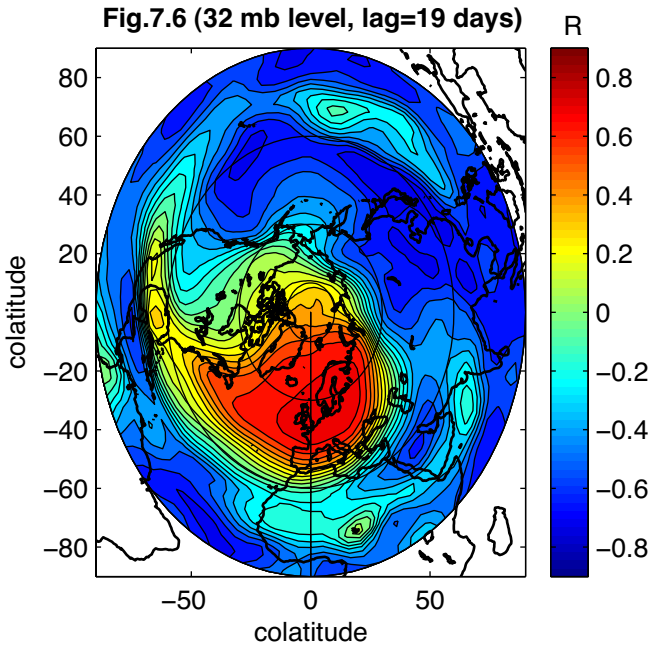

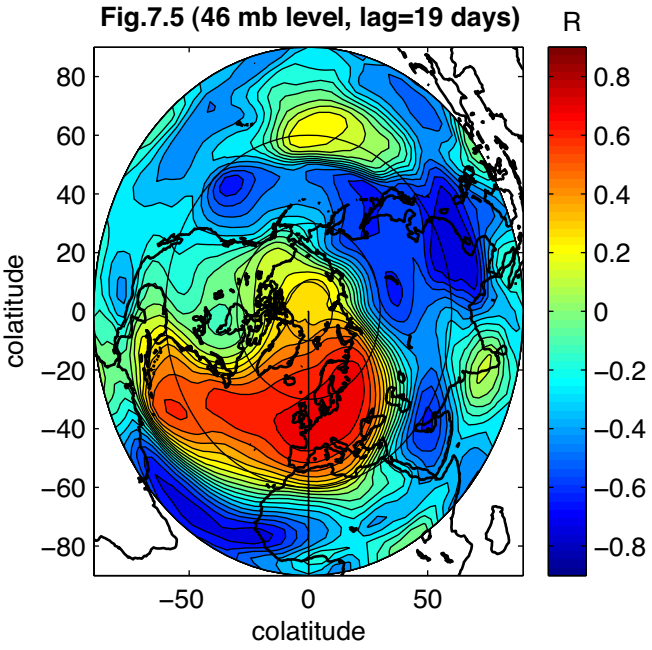

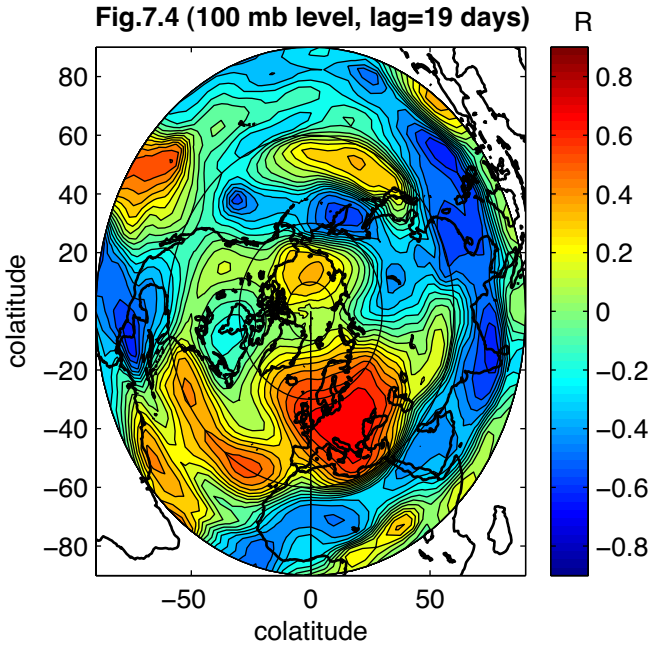

Correlation maps of the 8−day low−pass filtered temperature data at location around the North Hemisph. at 10−100 mb and with that at Abisko at 1000 mb with lag of 20−19 days back for the period December 2002 − February 2003.

Fig.7.8.1 (3.2 mb level, lag=52 days)

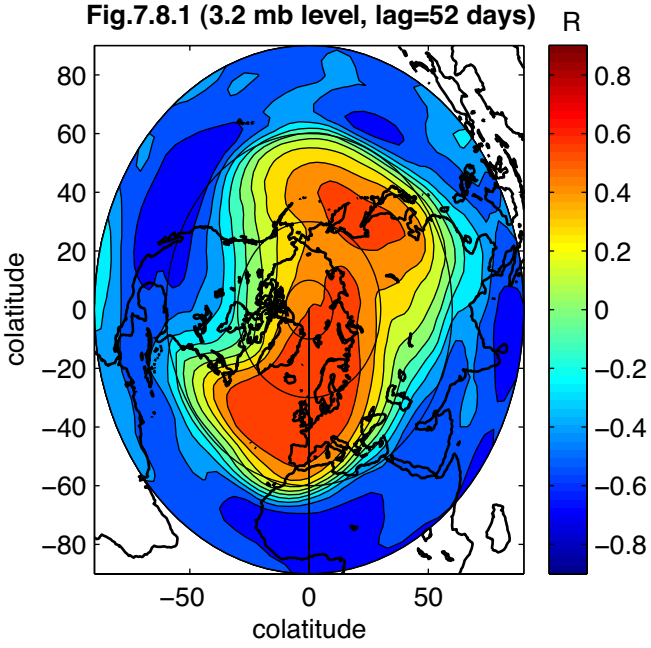

Fig.7.8.2 (3.2 mb level, lag=21 days)

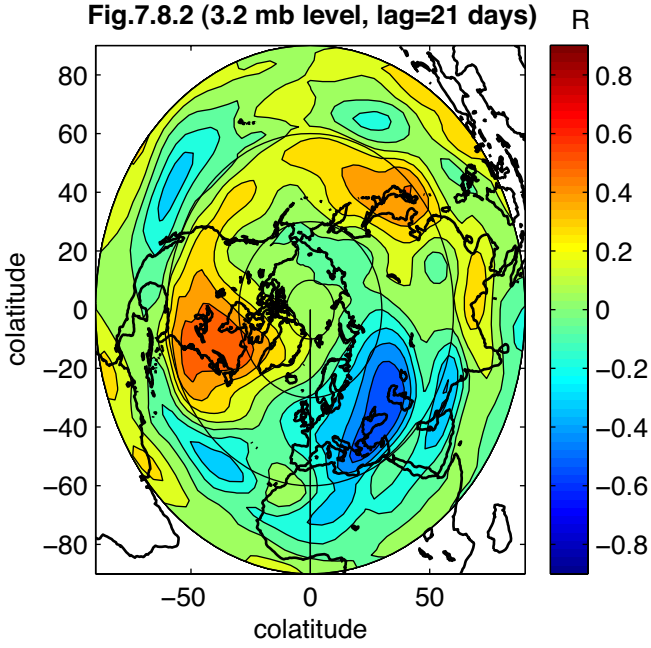

Fig.7.7.1 (10 mb level, lag=52 days)

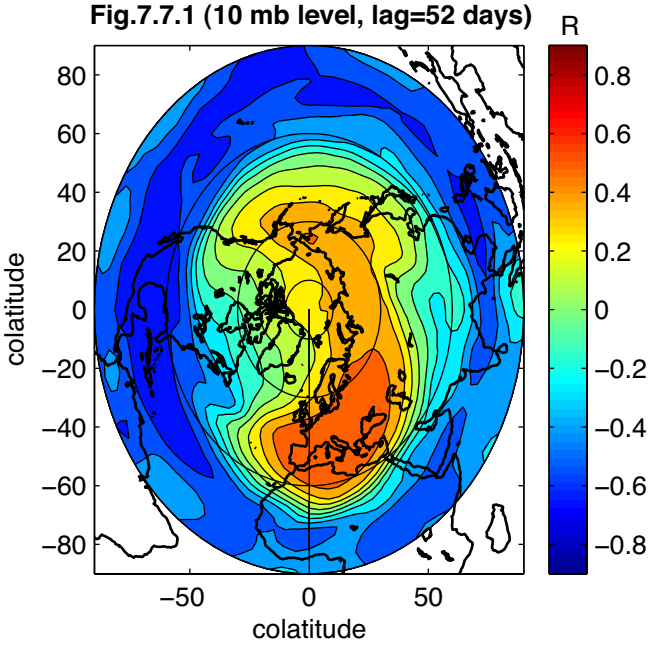

Correlation maps of the 8−day low−pass filtered temperature data at location around the North Hemisph. at 3.2−10 mb and with that at Abisko at 1000 mb with lag of 52 and 21 days back for the period December 2002 − February 2003.

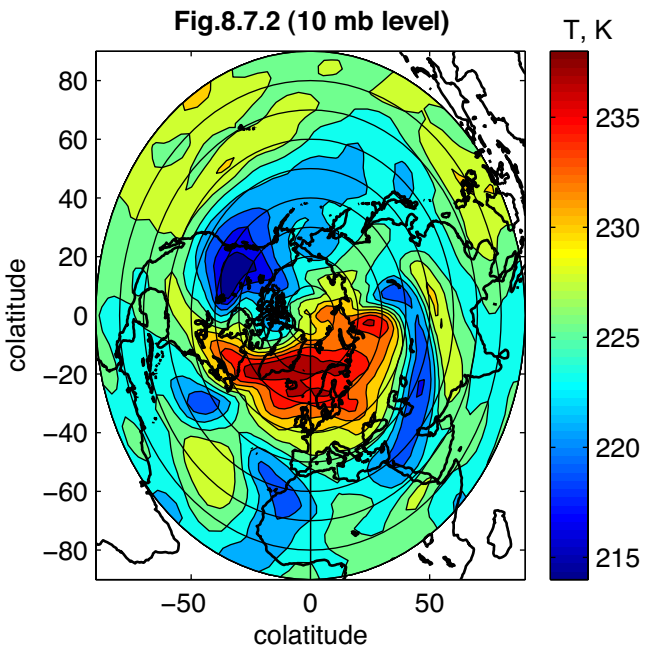

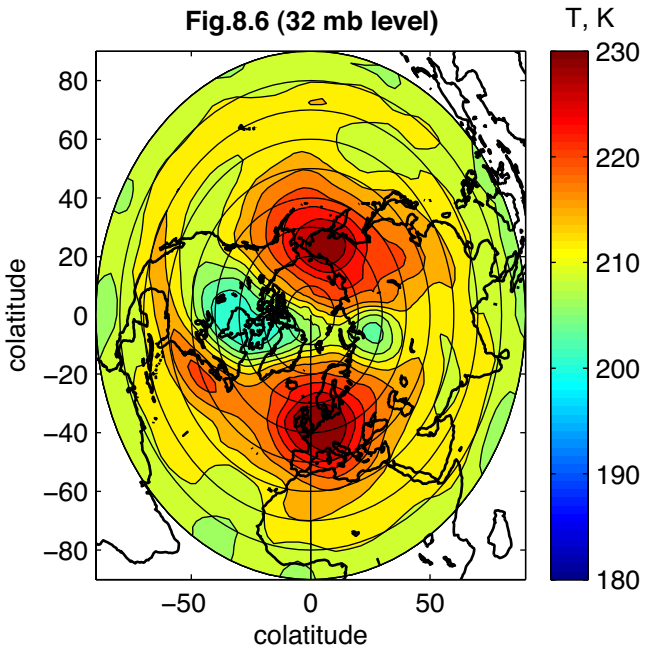

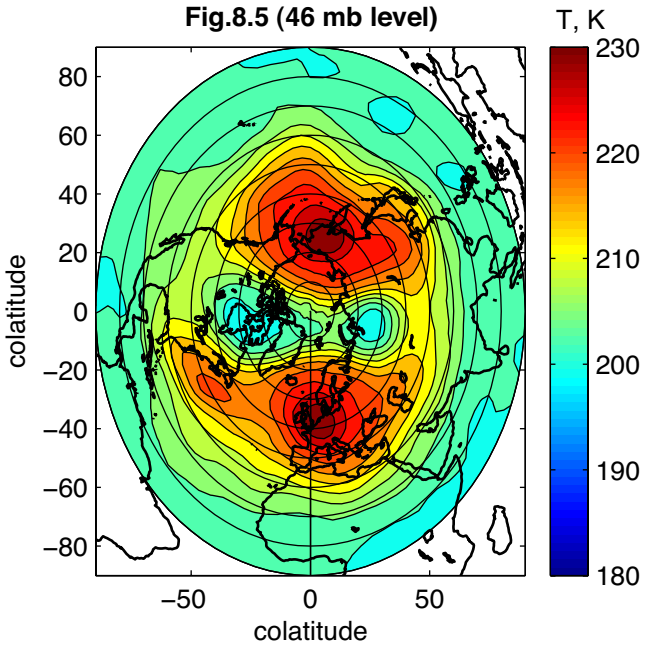

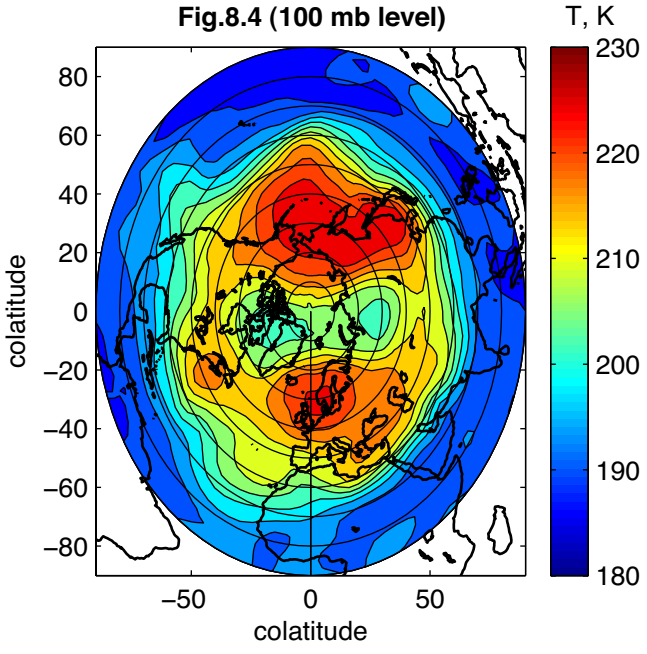

Temperature maps on 28 January 2003 (19 days back from 16 February when there was the warmest day in Kiruna in winter 2002/2003)

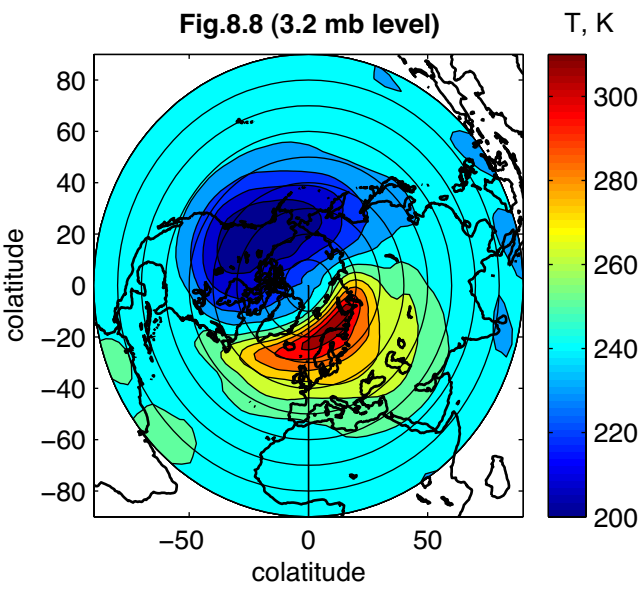

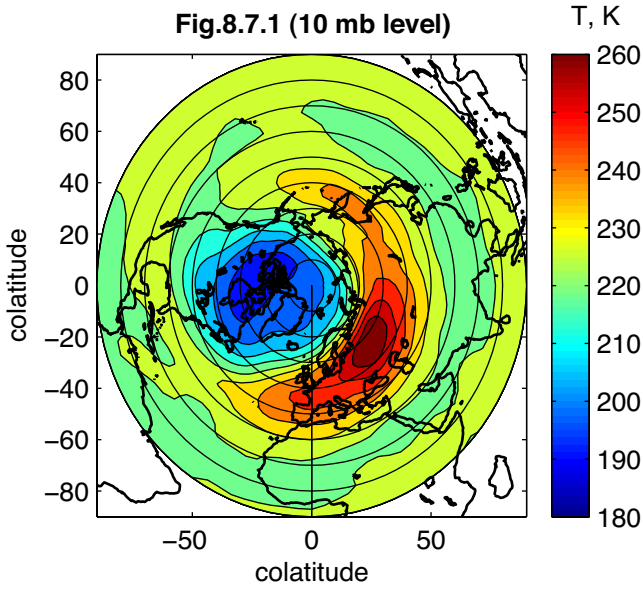

Temperature maps on 26 December 2002 (52 days back from 16 February 2003 when there was the warmest day in Kiruna in winter 2003/2003)